Physics – Uspekhi **58** (7) 701 – 718 (2015)

PHYSICS OF OUR DAYS PACS numbers: 41.75.Ak, 41.85.Ar, 52.25.Jm, 52.40.Kh, 52.59.Bi, 52.59.Sa, **52.65. – y**

Theory of a plasma emitter of positive ions

I A Kotelnikov, V T Astrelin

DOI: 10.3367/UFNe.0185.201507c.0753

Contents

Abstract. The results obtained to date by the one-dimensional theory of the emission of positive ions by a plasma are reviewed from a unified point of view. Simple and generalized forms of the Bohm criterion are discussed. The unipolar sheath model and the two-scale theory are outlined. Kinetic and hydrodynamic models for the formation of the Debye sheath and of the ionization zone in the presheath are described. It is shown that, except for some artificial ionization models, the Bohm criterion is fulfilled in the equality form. The emission current from the plasma emitter is calculated in the hydrodynamic and kinetic approximations. Existing numerical codes for the simulation of positive ion sources in two and three dimensions are briefly described.

Keywords: Bohm criterion, Debye sheath, unipolar sheath, space-charge-dominated beams, plasma simulation

1. Introduction

Only a limited number of papers in the Russian scientific literature provide reviews of ion sources. Examples from 20–40 years ago comprise monographs [1, 2] and *UFN* paper [3], respectively coauthored and authored by Gabovich, and a Russian translation of Forrester's book [4]. Kreindel's monograph [5] focuses on electron — but also touches on ion — emissions from plasma. In a recent monograph [6] by Koval' and coworkers, two chapters describe present-day plasma sources of electrons and ions and analyze some aspects of charged particle emission from a plasma. Other publications address specific aspects of this vast field and usually assume a basic knowledge by the reader of the theory of charged particle emission from plasma. The present paper makes an attempt at a unified description (with lacunas, if present, filled) of the theoretical results known to date on the emission of positive ions from plasma. The theory of the formation of electron and of negative ion beams in sources with a plasma emitter will be left out of our discussion.

Let us first clarify the concept of a plasma emitter. We consider the plasma emitter as a construction element of an ion source, and the ion source as a device for producing ion beams. The plasma emitter replaces the solid state emitter, for example, the thermionic cathode in an electron source. In a source with a plasma emitter, charged particles are drawn from a plasma with a free boundary whose shape and position are not known *a priori*.

On the other hand, we consider the plasma emitter to be an object of physical research. According to Refs [2, p. 10] and [6, p. 529], a *plasma emitter* is most simply described (neglecting neutral atoms) as a homogeneous mixture of an electron gas and an ion gas with approximately equal concentrations. This, however, is a very simplistic first-approximation definition. We will see that there are two components which should be considered as integral to the plasma emitter: the Langmuir sheath on the side of the charged particle collector (or the accelerating electrode), and

I A Kotelnikov, V T Astrelin Budker Institute of Nuclear Physics, Siberian Branch of the Russian Academy of Sciences,
prosp. Akademika Lavrent'eva 11, 630090 Novosibirsk, Russian Federation;
Novosibirsk State University,
ul. Pirogova 2, 630090 Novosibirsk, Russian Federation
E-mail: I.A.Kotelnikov@inp.nsk.su, V.T.Astrelin@inp.nsk.su

Received 26 March 2015, revised 7 May 2015
Uspekhi Fizicheskikh Nauk **185** (7) 753 – 771 (2015)
DOI: 10.3367/UFNr.0185.201507c.0753
Translated by E G Strel'chenko; edited by A Radzig

the ionization region deep inside the plasma, where the plasma is of necessity inhomogeneous.

The basis of the theory of a plasma emitter is the well-known Bohm criterion [7], which determines the necessary condition for the formation of a Debye sheath at the boundary of quasineutral plasma. Its derivation, to be found in classical textbooks [4, 8–13] and reviews [14], assumes the presence of a Debye sheath which arises near an electrode immersed in the plasma. The origins of plasma physics as a science can be traced to the study by Langmuir and coworkers of gas discharge phenomena that form a charged sheath near such an electrode [15–19]. Today, the Bohm criterion is a curriculum topic for any undergraduate student interested in probe measurements in plasma [20–24].

The method invoked in deriving the Bohm criterion is quite applicable to a description of the plasma emitter of positive ions, a device which has recently become very important for the development of high-current sources of charge particles and neutral atoms. A corresponding — and quite obvious — generalization of Bohm's theory is discussed in Chen's book [10], which does not mention the plasma emitter though — unlike monograph [2] by Gabovich and coworkers, with a special section devoted to the plasma emitter of positive ions.

Following the terminology of Riemann and Tsendin [25], the Debye sheath on the plasma surface is separated from the ion collector by a unipolar sheath whose potential approximately obeys the Child – Langmuir law [26, 27]. The Debye and unipolar sheaths combined form the so-called *Langmuir sheath* [25, 28]. The exact boundary between the Debye and unipolar sheaths defies a rigorous definition. The Debye sheath changes smoothly into the unipolar sheath over a few Debye lengths. As for the qualitative difference between them, in the unipolar sheath the electron density is negligibly small compared to — is, say, less than two percent of — the positive ion density, whereas the ion and electron densities in the Debye sheath are of the same order of magnitude. As for the boundary between the quasineutral plasma and the Debye sheath, it can be defined with a sufficient rigor applying the two-scale theory [29–33].

In this theory, the smaller and larger scales are those of the Debye length λ_D and of the ionization zone thickness L, respectively. In the ionization zone, which is more often referred to — but is not always the same as — the Debye presheath, plasma can usually be considered quasineutral. In the Debye sheath, with its marked departure from quasineutrality, ionization can be neglected, assuming that the ion current arising in the ionization zone remains unchanged. Bohm's theory is formulated for the Debye sheath. On the scale of the ionization zone, the Debye sheath appears as a mathematical singularity which arises due to the Poisson equation being replaced by the quasineutrality condition.

The regular Bohm solution for the Debye sheath is matched with the singular solution for the ionization zone at a distance of $\delta z_D = \lambda_D^{1-\beta} L^{\beta}$ from the singularity, with $\beta = 1/5$ in the hydrodynamical model, and $\beta = 1/9$ in the kinetic theory. If measured in units of λ_D, in the limit of $\lambda_D/L \to 0$ the distance to the matching point, $\delta\xi_D = \delta z_D/\lambda_D = L^{\beta}/\lambda_D^{\beta}$, moves off to infinity. Therefore, Bohm's theory assumes that the ion flow is specified at an infinite distance from the Debye sheath. If, on the other hand, the distance is measured in units of L, then in the same limit the Debye sheath width $\delta s_D = \delta z_D/L = \lambda_D^{1-\beta}/L^{1-\beta}$ tends to zero, and the sheath itself degenerates into a singularity.

The analytical theory of the plasma emitter is limited by the one-dimensional case. A one-dimensional theory is intended to help in formulating the boundary conditions for numerical codes that are applied in calculating real-life charge particle sources. In high-current sources, the Debye length is often too small compared to the device size for the numerical codes to resolve it; therefore, the real potential distribution near the free plasma surface is replaced in some codes by model boundary conditions between the quasineutral plasma and the unipolar sheath with a transitional zero-thickness Debye sheath. The free plasma surface (free meaning no contact with a solid electrode) is in the present context called the emission surface or plasma *meniscus* (see, for example, monograph [13]).

The paper outline is as follows. In Section 2, we start introducing the theory of the plasma emitter of positive ions by first deriving the Bohm criterion in the hydrodynamic approximation. The basic concepts of the theory, such as the Debye, unipolar, and Langmuir sheaths, are defined in Section 3. The unipolar sheath is described in Section 4. The two-scale theory is formulated in Section 5. Section 6 considers hydrodynamic models of the ionization zone in the Debye presheath. A kinetic generalization of the Bohm criterion is formulated in Section 7. A kinetic model of the ionization zone is described in Section 8. Section 9 presents a model of a spatially localized ion source. In Section 10, the calculation of the emission current from the surface of a plasma emitter is performed. Section 11 lists some of the existing numerical codes for modeling ion sources in two and three dimensions. Section 12 discusses the shape of a plasma emitter in a two-dimensional geometry. Finally, the basic conclusions are arrived at Section 13.

2. Bohm's criterion

To obtain the Bohm criterion in its original formulation, we make use of the system of equations for two-fluid hydrodynamics supplemented by the Poisson equation:

$$\frac{\partial}{\partial z} n_e v_e = 0 , \tag{1a}$$

$$\frac{\partial}{\partial z} n_i v_i = 0 , \tag{1b}$$

$$\frac{\partial}{\partial z} m_e n_e v_e^2 = -\frac{\partial}{\partial z} n_e T_e + e n_e \frac{\partial \varphi}{\partial z} , \tag{1c}$$

$$\frac{\partial}{\partial z} m_i n_i v_i^2 = -\frac{\partial}{\partial z} n_i T_i - e n_i \frac{\partial \varphi}{\partial z} , \tag{1d}$$

$$\frac{\partial^2 \varphi}{\partial z^2} = 4\pi e (n_e - n_i) . \tag{1e}$$

Here, $e > 0$ denotes the elementary charge, v_e and v_i are the electron and ion flow velocities, respectively; the remaining notation is conventional.

We will assume that electrons are, on average, at rest, so that $v_e = 0$. But even if the electron and ion flow velocities, v_e and v_i, are of the same order of magnitude, the electron kinetic energy $m_e v_e^2/2$ is small compared to the ion kinetic energy $m_i v_i^2/2$ due to the huge difference between m_e and m_i, allowing the left-hand side of Eqn (1c) to be set equal to zero. Then, from this equation it follows that the electron density obeys the Boltzmann distribution

$$n_e = n_0 \exp\left(\frac{e\varphi}{T_e}\right) , \tag{2}$$

where n_0 is the electron number density in the quasineutral region, whose potential we will consider to be zero. We are looking for a solution that describes a plasma emitter of ions, assuming that $\varphi \to 0$ and $\partial\varphi/\partial z \to 0$ deep in the plasma for $z \to -\infty$ and that, outside of the plasma region, for $z \to +\infty$ the potential tends to $-\infty$ according to the Child–Langmuir (three halves) law — similar to a diode with emission limited by a space charge, where $\varphi \propto -z^{4/3}$ [26, 27].

Following D Bohm, let us consider the case in which the ion temperature T_i is so much less than the electron temperature T_e that it can be neglected. Then, using Eqns (1b) and (1d), we easily find the ion velocity and ion number density as functions of the electric potential φ, the former being given by

$$v_\mathrm{i} = \sqrt{v_0^2 - 2e\varphi/m_\mathrm{i}}\,, \tag{3}$$

and the latter by

$$n_\mathrm{i} = \frac{n_0 v_0}{\sqrt{v_0^2 - 2e\varphi/m_\mathrm{i}}}\,, \tag{4}$$

where v_0 is the ion velocity at $\varphi = 0$. Next we substitute Eqns (2) and (4) into the Poisson equation (1e) and change to the dimensionless variables

$$\xi = \frac{z}{\lambda_\mathrm{D}}\,, \quad \chi = \frac{e\varphi}{T_\mathrm{e}}\,, \quad u_0 = \frac{v_0}{c_\mathrm{s}}\,, \tag{5}$$

where $\lambda_\mathrm{D} = \sqrt{T_\mathrm{e}/4\pi e^2 n_0}$ is the Debye length, and $c_\mathrm{s} = \sqrt{T_\mathrm{e}/m_\mathrm{i}}$ is the ion speed of sound. The equation

$$\frac{\mathrm{d}^2\chi}{\mathrm{d}\xi^2} = \exp(\chi) - \frac{u_0}{\sqrt{u_0^2 - 2\chi}} \equiv -\frac{\partial U}{\partial\chi} \tag{6}$$

obtained in this way admits a useful mechanical analogy with an imaginary quasiparticle which moves in the field of the effective potential

$$U(\chi) = 1 - \exp(\chi) - u_0\sqrt{u_0^2 - 2\chi} + u_0^2\,, \tag{7}$$

where ξ has the meaning of time, and χ is the pseudoparticle coordinate. The mechanical energy of such a pseudoparticle is an integral of motion:

$$W = \frac{1}{2}\left(\frac{\mathrm{d}\chi}{\mathrm{d}\xi}\right)^2 + U(\chi) = \text{const}\,. \tag{8}$$

Assuming that for $\xi \to -\infty$ both the coordinate χ and velocity $\mathrm{d}\chi/\mathrm{d}\xi$ of the pseudoparticle vanish, we find that the constant in Eqn (8) is zero. Hence, it follows that

$$\frac{1}{2}\left(\frac{\mathrm{d}\chi}{\mathrm{d}\xi}\right)^2 = \exp(\chi) - 1 + u_0\sqrt{u_0^2 - 2\chi} - u_0^2\,. \tag{9}$$

In the limit of $\chi \to 0$, this equation can be simplified by applying the Taylor expansion of its right-hand side near $\chi = 0$:

$$\frac{1}{2}\left(\frac{\mathrm{d}\chi}{\mathrm{d}\xi}\right)^2 \approx \left(\frac{1}{2} - \frac{1}{2u_0^2}\right)\chi^2\,. \tag{10}$$

Because the left-hand side of Eqn (10) is nonnegative, a solution exists if the right-hand side is also nonnegative, i.e.,

$$u_0^2 \geqslant 1\,. \tag{11}$$

Notably, the solution which decreases with increasing ξ has the form

$$\chi = \chi_s \exp\left(\sqrt{1 - \frac{1}{u_0^2}}\,(\xi - \xi_s)\right), \tag{12}$$

where $\chi_s < 0$, and ξ_s are certain constants whose meaning will be made clear in Section 3. In dimensional variables, this solution describes the variation of the electric potential

$$\varphi = -\frac{|\chi_s|\,T_\mathrm{e}}{e}\exp\left(\sqrt{1 - \frac{1}{u_0^2}}\,\frac{z - z_s}{\lambda_\mathrm{D}}\right)$$

from zero deep in the plasma (for $z \to -\infty$) to small negative values close to its boundary ($z \to z_s$).

At the other extreme, $\chi \to -\infty$, we have

$$\frac{1}{2}\left(\frac{\partial\chi}{\partial\xi}\right)^2 = u_0\sqrt{-2\chi}\,, \tag{13}$$

which gives

$$\chi = -\left(\frac{u_0^2}{2}\right)^{1/3}\left(\frac{3\xi}{2}\right)^{4/3}, \tag{14}$$

i.e., for $z \to +\infty$, one finds

$$\varphi = -\frac{T_\mathrm{e}}{e}\left(\frac{u_0^2}{2}\right)^{1/3}\left(\frac{3z}{2\lambda_\mathrm{D}}\right)^{4/3}.$$

The last expression, when rewritten as

$$j_{3/2} = en_0v_0 = \frac{\sqrt{2e}}{9\pi\sqrt{m_\mathrm{i}}}\,\frac{|\varphi|^{3/2}}{z^2}\,, \tag{15}$$

shows that outside of the plasma the current density obeys the Child–Langmuir law. In the approximation specified by Eqn (15), it does not depend on the electron temperature T_e.

A formal solution of Eqn (9), for which $\chi = \chi_p$ at $\xi = \xi_p$, can be written down in an implicit form as

$$\xi - \xi_p = -\int_{\chi_p}^{\chi} \frac{\mathrm{d}\chi}{\sqrt{2}\sqrt{\exp(\chi) - 1 + u_0\sqrt{u_0^2 - 2\chi} - u_0^2}}\,. \tag{16}$$

With condition (11) satisfied, formula (16) defines a single-valued monotonically decreasing function $\chi(\xi - \xi_p)$. This function is plotted in Fig. 1 for several values of u_0^2 at $\chi_p = -4$ and $\xi_p = 0$. The corresponding plots of ion and electron number densities are shown in Fig. 2.

Written in terms of dimensional quantities, the meaning of condition (11) is that the ion velocity in the quasineutral region is greater than or equal to the ion speed of sound:

$$v_0 \geqslant c_\mathrm{s}\,. \tag{17}$$

This condition is known as *Bohm's sheath criterion* [4, 10–13, 30], although Bohm himself called it "a criterion for the stability of a sheath" [7, 34]. If Bohm's criterion is not met, then it was shown [35] that a rarefaction wave [36] forms, which propagates opposite to the ion flow toward the source region and interferes with the source there. How the discovery of the Bohm criterion was made and what events preceded and followed it are described in Allen's paper [37].

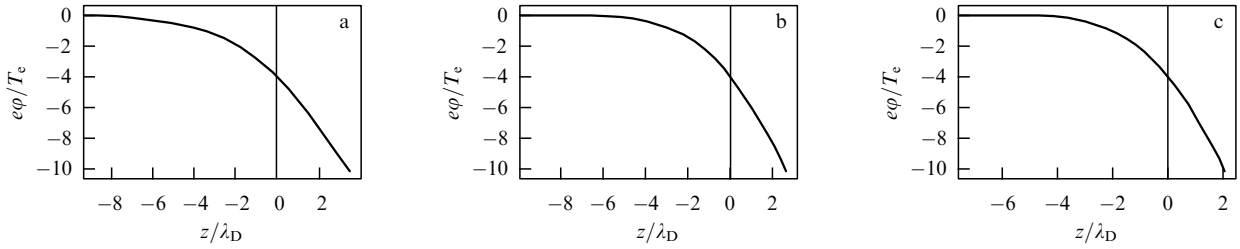

Figure 1. Potential profile near a plasma emitter for different values of the parameter u_0^2: (a) $u_0^2 = 1$, (b) $u_0^2 = 2$, and (c) $u_0^2 = 10$; $\chi_p = -4$, $\xi_p = 0$.

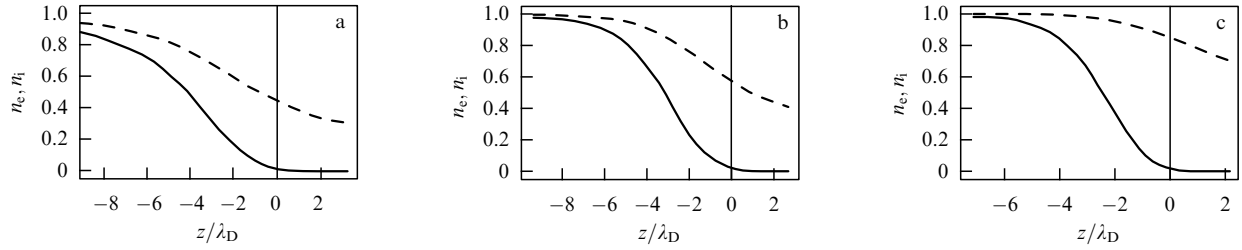

Figure 2. Electron (solid lines) and ion (dashed lines) number densities near a plasma emitter for different values of the parameter u_0^2: (a) $u_0^2 = 1$, (b) $u_0^2 = 2$, and (c) $u_0^2 = 10$; $\chi_p = -4$, $\xi_p = 0$.

3. Debye sheath

The problem discussed in Section 2 and concerned with the potential profile at the boundary of a collisionless plasma presents a difficulty in that some of the terms it involves are given different interpretations in the literature. That part of the charged layer at the plasma boundary where the electron and ion number densities, although order-of-magnitude similar, are not even approximately equal is referred to as the *Debye sheath* (see, for example, Ref. [25]). The common belief is that the Debye sheath has a thickness of a few Debye lengths (see, for example, Ref. [38]) and that the Debye length is much smaller than other characteristic dimensions, which is exactly the reason why the Debye sheath can be considered collisionless. Within this sheath, the dimensionless electric potential χ is negative, and its absolute value varies from fractions to several units. The exact boundaries of the Debye sheath are not defined within Bohm's theory. In what follows, we will stipulate that the interval

$$-4 < \chi < 0 \tag{18}$$

corresponds to the Debye sheath. At the top of this interval, for $\chi \to 0$, the plasma becomes quasineutral in the sense that $n_e \approx n_i \approx n_0$; however, asymptotic form (12) does not hold true and cannot explain how the supersonic ($v_0 \geqslant c_s$) ion flow formed. A consistent theory should take into account particle collision and ionization processes that occur in the neutral gas and actually form this flow, whereas in Bohm's theory the plasma is considered collisionless, which is expressed in the fact that the right-hand sides of equations (1a) and (1b) are zero.

If plasma ions are created with small velocities, they are accelerated to the Bohm criterion velocity by the electric field in the *ionization zone*, where a positive electric potential forms. It is this potential in the ionization zone which gives rise to the formation of an ion flow at the boundary of the quasineutrality zone in front of the entrance to the Debye sheath at $\chi \approx 0$, whereas in Bohm's theory this flow is considered to be specified as a boundary condition for $\xi \to -\infty$. Because according to the Bohm criterion (17) the ion velocity v_0 at the entrance to the Debye sheath should, as a minimum, reach the speed of sound $c_s = \sqrt{T_e/m_i}$, it follows that the drop in the potential energy $e\varphi$ in the ionization zone is, as a minimum, equal to $m_i c_s^2/2 = T_e/2$, i.e., in the ionization zone we have

$$0 < \chi < \frac{1}{2}\,. \tag{19}$$

Following Refs [25, 30, 32, 39], we will also apply the term *Debye presheath* when referring to the ionization zone, although this term is sometimes used to denote the 'transition region' between the Debye sheath and the quasineutral plasma [33, 40]. The Debye presheath is quasineutral. In probe measurements made in a preliminary ionized plasma, the presheath around the (most often cylindrical) probe is formed by Coulomb collisions and its size is determined by the ion mean free path; in this paper, however, we neglect Coulomb collisions. The theory of the presheath presented in Sections 6 and 8 predicts that its upper boundary $\chi = \chi_{pl}$ in fact exceeds the value of 1/2 and approaches unity. We will label by 'pl' the quantities referring to this boundary, having in mind that they characterize the parameters of the quasineutral plasma outside of the presheath.

Finally, when referring to the region

$$\chi < -4 \tag{20}$$

on the opposite side of the Debye sheath, we will, following Ref. [25], use the term *unipolar sheath*; this is a region where the Child–Langmuir law [26, 27] holds approximately. The unipolar and Debye sheaths together form the *Langmuir sheath*, which Riemann calls the Langmuir–Debye sheath [25, 28], and Lieberman and Lichtenberg call the Child law sheath [11].

The value of $\chi = \chi_p = -4$ at the interface between the Debye and unipolar sheaths was chosen to ensure that the electron density does not exceed $\exp(\chi_p) \approx 2\%$ of n_0 anywhere in the unipolar sheath. This value is used in determin-

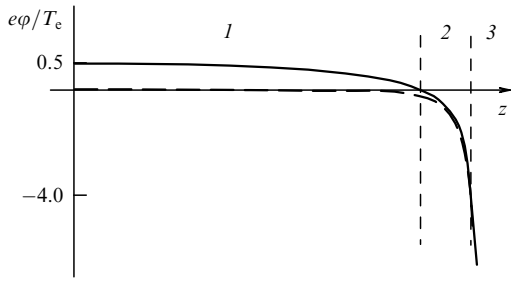

Figure 3. One-dimensional model of a plasma emitter: *1*, quasineutral ionization zone (Debye presheath), $0 < e\varphi/T_e < 1/2$; *2*, Debye sheath, $-4 < e\varphi/T_e < 0$ (the Debye sheath length is usually much less than shown), and *3*, unipolar sheath, $e\varphi/T_e < -4$; solid line is the potential profile in the two-scale theory, dashed line is the Bohm solution, which is invalid in region *1*.

ing the emission surface in certain numerical codes and is close to the value of $\chi \approx -\ln\sqrt{m_i/m_e} \approx -3.8$ for which the ion current in a hydrogen plasma becomes comparable to the electron current onto the probe with a floating potential. Throughout what follows, we will mark by the subscript p the quantities that refer to the Debye–unipolar sheath interface; for example, z_p denotes the coordinate z at this boundary, and ξ_p is the value of the dimensionless variable $\xi = z/\lambda_D$.

The different regions of the plasma emitter of positive ions are shown schematically in Fig. 3, where the quasineutral region immediately borders the Debye sheath. In Section 9, we will discuss an example which features a formation in the ionization zone of a second Debye sheath, separated from the Langmuir sheath by an extended quasineutral region in which the potential is everywhere approximately zero.

Finally, let us identify the position $\chi = \chi_s$ of the applicability boundary of Bohm's theory in the $\chi \to 0$ limit. We will use the subscript s to label the quantities referring to this boundary. If we assume that $\chi_s \to 0$, then the Debye sheath thickness $\delta\xi_D = \xi_p - \xi_s$ calculated by comparing the exact solution (16) with the asymptotic form (12) tends to infinity, which sets considerable difficulties before the theory, because the ion mean free path is finite and collisions in an infinite plasma sheath cannot be neglected (as they were in Bohm's theory). The two-scale theory to be outlined in Section 5 gives a reasonable definition of the boundary χ_s by interpreting the Debye sheath thickness $\delta z_D = z_p - z_s$ as a length which is larger than the Debye length, $\delta z_D \gg \lambda_D$, but which, however, tends to zero, $\delta z_D \to 0$, if $\lambda_D \to 0$. The Debye sheath in this theory can be considered collisionless, whereas in the quasineutral zone one should take into account neutral gas ionization and Coulomb collision processes. In this sense, $\chi = \chi_s$ is the boundary between the Debye sheath and quasineutral presheath.

Recalling our assertion earlier in this section that this boundary is $\chi = 0$, we see now that this was just the first approximation. The exact value of the parameter χ_s is close to zero and is important when calculating the Debye thickness but not the plasma density or the ion flow velocity, which vary negligibly between $\chi = 0$ and χ_s points in the plasma. In this sense, the first approximation was not that bad after all.

4. Unipolar sheath

As our further discussion will show, the Bohm criterion (17) is usually satisfied in the form of an equality [25, 30, 31, 37, 41, 42]. Such, at least, is the conclusion suggested by the theory presented in Sections 6 and 8, which assumes that the ionization zone greatly exceeds the Debye length and is therefore quasineutral. The consequence is that the Debye sheath at the boundary of a plasma emitter of ions bears a universal character, i.e., of the three ion and electron number density profiles shown in Fig. 2a–c, only 2a is realized. Hence, $v_0 = c_s$, and the emission current $j_p = en_0v_0$ has a strictly defined value:

$$j_p = en_0c_s\,. \tag{21}$$

In Section 10, we will see that this equation acquires in kinetic theory a numerical coefficient close to unity. Anyway, the emission current is determined by the processes occurring in the ionization zone, for example, by the neutral gas supply rate and radio-frequency (RF) heating power. Accordingly, the plasma density $n_0 = j_p/ec_s$ at the edge of the quasineutral zone in front of the entrance to the Debye sheath is uniquely determined by the magnitude of the emission current j_p, whereas in Bohm's theory outlined in Section 4 the plasma density n_0 is, on the contrary, considered a free parameter.

If a large negative voltage $|U| \gg T_e/e$ is applied to the ion collector electrode, an electron-free *unipolar ion sheath* forms behind the Debye sheath. In the collisionless case, its thickness is obtained from Eqn (15) by substituting $z = d$ and $\varphi = U$ to give

$$j_{3/2} = \frac{\sqrt{2e}}{9\pi\sqrt{m_i}}\,\frac{|U|^{3/2}}{d^2}\,. \tag{22}$$

Known in this form as the Child–Langmuir law [26, 27] or as the 'three halves' law, this equation relates three quantities: the current in the planar diode with the emission limited by a space charge; the specified value d of the electrode–electrode gap, and the specified value of the applied voltage U. As applied to the plasma emitter, the meaning of relation (22) is completely different. Here, the emission current $j_p = en_0c_s$ is determined by processes inside the plasma, and the variable quantity is the gap d between the emitter surface and the ion collector: at a specified voltage U, the plasma fills all the accessible space, leaving a gap of the desired size before the collector. Combining Eqns (21) and (22) at $j_p = j_{3/2}$ yields

$$d = \frac{\sqrt{2}}{3}\left(\frac{2e|U|}{T_e}\right)^{3/4}\lambda_D\,. \tag{23}$$

For $d/\lambda_D \gg 1$, there are reasons for modeling the plasma emitter as an emission surface on which the electron density jumps down to zero [43, 44]. If the Debye sheath thickness (on the order of a few λ_D) is small compared to the unipolar sheath width d, the electron density could presumably be represented by a step function. Setting the electric field and initial ion velocity to zero at the edge of the step at $z = 0$, we obtain the Child–Langmuir law (22). This law, however, gives only an approximate, rough picture of the unipolar sheath.

Riemann and Tsendin [25] offered a more accurate description. Following their treatment, we start by substituting $u_0 = 1$ into Eqn (9) to obtain

$$\frac{1}{2}\left(\frac{d\chi}{d\xi}\right)^2 = \exp(\chi) - 2 + (1 - 2\chi)^{1/2}\,. \tag{24}$$

Neglecting the electron density, i.e., dropping the term $\exp(\chi)$ which is small for $\chi \to -\infty$, we obtain the equation

$$\frac{d\chi}{d\xi} = -\sqrt{2(1-2\chi)^{1/2} - 4}\,. \tag{25}$$

It has been possible to integrate yielding the potential in the unipolar sheath in the implicit form

$$\xi - \xi_p = \frac{\sqrt{2}}{3}\sqrt{\sqrt{1-2\chi} - 2}\left(\sqrt{1-2\chi} + 4\right). \tag{26}$$

Formula (26) correctly takes into account both the initial ion velocity and the integral contribution of electrons to the space charge. The error due to neglecting the contribution from those electrons present in the unipolar sheath is exponentially small. The Child–Langmuir limit

$$\xi - \xi_p = \frac{\sqrt{2}}{3}(-2\chi)^{3/4} \tag{27}$$

is obtained from formula (26) by dropping terms of order $\chi^{-1/2}$ as against unity.

The accuracy of the unipolar approximation is illustrated in Fig. 4, where the plot of formula (26) is compared both with the exact numerical solution of equation (24) and with the Child–Langmuir formula (27). The unipolar potential terminates at $\chi = -3/2$ because, for $\chi > -3/2$, the expression on the right-hand side of Eqn (26) becomes complex-valued. For $\chi < -2$, given the scale of the figure, the potential is virtually undistinguishable from that given by the exact solution. Reference [25] suggests $\chi = -2.303$ (at which $n_e = 0.1n_0$) as the boundary between the Debye and unipolar sheaths. For us, however, the boundary between above sheaths is best to be set at $\chi = \chi_p = -4$, corresponding to the electron number density $n_e \approx 0.018\,n_0$; such a potential is marked by a horizontal dashed–dotted line in Fig. 4.

It is interesting to note that, changing to dimensional variables, expression (25) at $\chi = \chi_p = -4$ takes the form

$$\frac{E^2}{8\pi} = n_0 T_e\,. \tag{28}$$

The numerical code POISSON-2 to be described in Section 11.3 uses equality (28) as a boundary condition at the emission surface of the plasma emitter. This equality implies

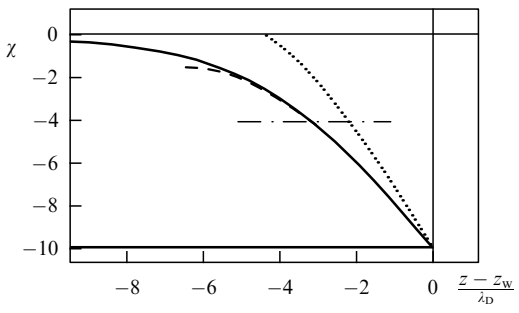

Figure 4. Potential profile in the Langmuir sheath: solid line, the exact solution of Eqn (24); dashed line, unipolar approximation (26); dotted line, the Child–Langmuir formula (27). Potential on the wall is always $\chi_w = -10$. The horizontal dashed–dotted line is the adopted boundary $\chi = -4$ between the unipolar and Debye sheaths.

that the electron pressure $n_0 T_e$ and the dynamic thrust of ions $n_i m_i v_i^2 = n_0 m_i c_s^2 = n_0 T_e$ from the inside of the Debye sheath (where $E \approx 0$) are balanced by the sum of the increased (due to the potential drop from $\varphi = 0$ to $\varphi = -4T_e/e$) dynamic thrust of ions, $n_i m_i v_i^2 = 3n_0 T_e$ [see Eqns (3) and (4)], and the negative electric field pressure (tension) $-E^2/8\pi$ from the outer side of the Debye sheath (where $n_e \approx 0$).

5. Two-scale theory

There was an early recognition by the pioneers of gas electronics for the distinction between quasineutral plasma and the thin near-electrode (Langmuir) sheath which produces a large volumetric charge density [15–19, 37, 45, 46]. If the electrode potential is large and negative, the near-electrode sheath can, in turn, be provisionally divided into the Debye sheath and the unipolar sheath described in Section 4. The Debye sheath typically has an estimated characteristic thickness of a few Debye lengths λ_D. Within it, the electron density falls by orders of magnitude, whereas in the unipolar sheath its value is already small compared to the ion density. It is therefore natural to consider that quasineutral plasma, whose size $L \gg \lambda_D$, has its 'edge' tied to the Debye sheath. On an intuitive level, this fact was formulated both by Bohm [7] and much earlier by Langmuir [15–19].

For a sufficiently small value of the ratio

$$\varepsilon = \frac{\lambda_D}{L}\,, \tag{29}$$

the boundary between the Debye sheath and the quasineutral plasma can be given a rigorous mathematical definition. The corresponding asymptotic (for $\varepsilon \to 0$) *two-scale theory* was developed early in the 1960s by Caruso and Cavaliere [29]. The papers by Riemann [28, 30–33] provided an easy-to-access description of the theory, and those by Franklin and Snell [47, 48] tested the theory by performing numerical calculations under various assumptions concerning the mean free path of particles in plasmas.

We will outline the theory by first introducing the ion source S_i into hydrodynamic equations (1) used in the derivation of the Bohm criterion and by assuming from the outset that $T_i = 0$. We have then a set of equations

$$n_e = n_0 \exp\left(\frac{e\varphi}{T_e}\right), \tag{30a}$$

$$\frac{\partial}{\partial z} n_i v_i = S_i\,, \tag{30b}$$

$$\frac{\partial}{\partial z} m_i n_i v_i^2 = -e n_i \frac{\partial \varphi}{\partial z}\,, \tag{30c}$$

$$\frac{\partial^2 \varphi}{\partial z^2} = 4\pi e(n_e - n_i)\,. \tag{30d}$$

Without loss of generality, we again believe that potential zero ($\varphi = 0$) and the normalization density n_0 refer to the 'onset' of the Debye sheath, where $n_e = n_0$. In writing down equations (30), it was assumed that the source of ions injects them into the plasma with a zero initial velocity, so that the continuity equation (30b) contains an $S_i(z)$ term, whereas the equation of motion (30c) does not. A common assumption in theoretical work is that the ion source intensity S_i is independent of, proportional to, or varies as the square of the electron density n_e depending, respectively, on whether the ionization is by an RF field, by electron impact, or by

electron impact from an excited state. In this case $S_i = S_q n_e^q$, where S_q is a constant, and $q = 0$, 1, or 2 for these three mechanisms of ionization, respectively.

Equations (30) involve two 'natural' scales: the Debye length $\lambda_D = (T_e/4\pi n_0 e^2)^{1/2}$, and the ionization length $L = c_s n_0/S_q n_0^q$. Introducing the dimensionless variables

$$\chi = \frac{e\varphi}{T_e}\,, \qquad u = \frac{v_i}{c_s}\,, \qquad n = \frac{n_i}{n_0}\,,$$

equations (30) reduce to the form

$$\frac{d}{d\xi}\, nu = \varepsilon \exp(q\chi)\,, \tag{31a}$$

$$\frac{d}{d\xi}\, nu^2 = -n\,\frac{d\chi}{d\xi}\,, \tag{31b}$$

$$\frac{d^2\chi}{d\xi^2} = \exp(\chi) - n\,, \tag{31c}$$

if the coordinate z is normalized to the Debye length:

$$\xi = \frac{z}{\lambda_D}\,, \tag{32}$$

or, alternatively, to the form

$$\frac{d}{ds}\, nu = \exp(q\chi)\,, \tag{33a}$$

$$\frac{d}{ds}\, nu^2 = -n\,\frac{d\chi}{ds}\,, \tag{33b}$$

$$\varepsilon^2\,\frac{d^2\chi}{ds^2} = \exp(\chi) - n\,, \tag{33c}$$

if one introduces another dimensionless coordinate

$$s = \frac{z}{L}\,. \tag{34}$$

Equations (31) and (33) are equivalent for a finite $\varepsilon > 0$, but tend to different limits as $\varepsilon \to 0$. In the *sheath representation*, with the corresponding system of equations (31), ε appears as a coefficient of the ion source in Eqn (31a). Dropping this term in the limit of $\varepsilon \to 0$ takes us back to Bohm's theory (see Section 2). In the *plasma representation* leaning upon the system of equations (33), ε enters the Poisson equation (33c). In the limit of $\varepsilon \to 0$, this equation reduces to the quasineutrality condition, which indicates that the ion and electron densities are approximately equal. The corresponding solution is discussed in Section 6.

6. Hydrodynamic ionization model

In this section, we will work out the solution to the set of equations

$$\frac{d}{ds}\, nu = \exp(q\chi)\,, \tag{35a}$$

$$\frac{d}{ds}\, nu^2 = -n\,\frac{d\chi}{ds}\,, \tag{35b}$$

$$n = \exp(\chi)\,, \tag{35c}$$

which follow from equations (33) in the limit of $\varepsilon = 0$. A point to note in retracing the derivation of these equations in Section 5 is that the ion velocity was assumed to be zero at the moment of ion injection into the plasma. Therefore, ions injected into plasma regions with different potentials differ in their acquired energies from the outset, with the consequence that their distribution function cannot be characterized by a zero temperature. In other words, the cold-ion plasma model defined by Eqns (35) is not fully self-consistent. Still, the model is of some methodological interest, and we will use it in this section. Attempts to include a finite ion temperature in the hydrodynamic approximation were made in Refs [39, 49, 50]. A more adequate kinetic model is discussed in Section 8.

Recall that the parameter q in equations (33) has different values depending on what mechanism ionizes the neutral gas injected into the system to maintain the emission current. If the ionization is effected by primary electrons or an RF field, the ionization rate is independent of the electron density and $q = 0$. If the ionization is dominated by electron impact, the ionization rate is proportional to n_e^1 and $q = 1$. Finally, when $q = 2$, the ionization occurs from an excited state when the number of excited atoms is proportional to the electron density.

System of equations (35) can be solved for any q, yielding the dependence of the coordinate s on the velocity u or potential χ in the form of a combination of hypergeometric functions. For integer values of q, these functions are expressed in terms of polynomials and elementary functions. The solutions for $q = 0, 1, 2$ are given in Ref. [51].

Combining equations (35b) and (35c), and adding the condition

$$u = 1 \quad \text{at} \quad \chi = 0 \tag{36}$$

which simply fixes the value of the potential at the location where the flow velocity reaches the speed of sound, as a preliminary we note that

$$\chi = \ln\frac{2}{1+u^2} \tag{37}$$

for any value of parameter q. Substituting this into Eqn (35a) and imposing the additional condition

$$u = 0 \quad \text{at} \quad s = 0 \tag{38}$$

which ties the coordinate origin $s = 0$ to the location where $u = 0$, it is found that

$$s = \frac{2^{1-q}u}{q-1}\left[q\,{}_2F_1\left(\frac{1}{2}\,, 1-q\,; \frac{3}{2}\,; -u^2\right) - (1+u^2)^{q-1}\right], \tag{39}$$

where ${}_2F_1$ denotes the hypergeometric function. In the cases of interest here, one finds

$$s = \frac{2u}{1+u^2} \qquad \text{at} \quad q = 0\,, \tag{40a}$$

$$s = 2\arctan(u) - u \qquad \text{at} \quad q = 1\,, \tag{40b}$$

$$s = \frac{1}{6}\,(3u - u^3) \qquad \text{at} \quad q = 2\,. \tag{40c}$$

The corresponding solutions are plotted in Fig. 5.

At $q = 0$, the s dependence of the potential and flow velocity can be written down in the explicit form

$$\chi = -\ln\left(\frac{1-\sqrt{1-s^2}}{s^2}\right), \quad u = \frac{1-\sqrt{1-s^2}}{s}\,. \tag{41}$$

At point $s \to s_p = 1$, where the flow velocity approaches the speed of sound, i.e., $u = 1$, the electric field $d\chi/ds$ and the

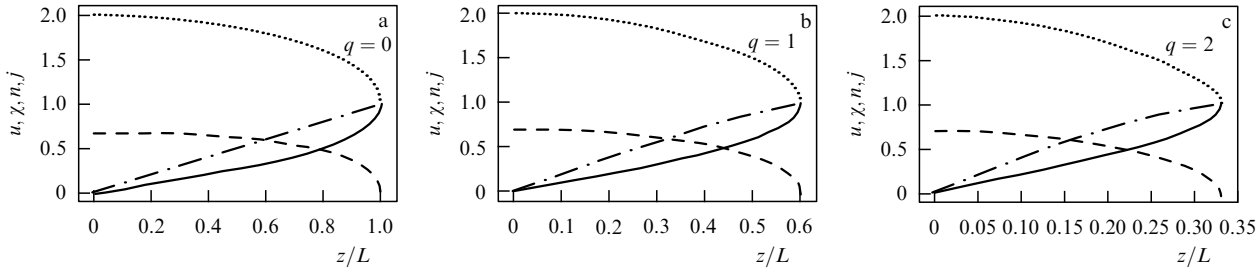

Figure 5. Flow velocity u (solid line), potential χ (dashed line), density n (dotted line), and ion flow $j = nu$ (dashed–dotted line) profiles for different values of the parameter q (shown in figures).

space charge $\varepsilon^2 \, \mathrm{d}^2\chi/\mathrm{d}s^2$ become infinite, with

$$\frac{\mathrm{d}\chi}{\mathrm{d}s} \approx -\frac{1}{\sqrt{2(s_p - s)}} \,. \tag{42}$$

This singularity corresponds to the Debye sheath in the exact solution, so that in the neighborhood of the singularity asymptotic solution (41) becomes meaningless. The coordinate s_s of the boundary between the quasineutral ionization zone ($s < s_s$) and the Debye sheath ($s > s_s$) can be determined by following the Riemann method [28]. At this boundary, the terms dropped in the quasineutral plasma model [namely, the space charge in Eqn (33c)]:

$$\varepsilon^2 \, \frac{\mathrm{d}^2\chi}{\mathrm{d}s^2} \sim \frac{\varepsilon^2}{(s_p - s_s)^{3/2}} \,,$$

and those dropped in Bohm's theory [namely, the correction to the ion density due to the supply from the ion source $\varepsilon \exp(q\chi)$ over the length $\delta\xi_\mathrm{D} = (s_p - s_s)/\varepsilon$ in Eqn (31a)]:

$$\delta n \sim \varepsilon \exp(q\chi) \frac{\delta\xi_\mathrm{D}}{u} \sim \varepsilon\delta\xi_\mathrm{D} \,,$$

make equal contributions.

From the equality $\varepsilon^2/(\delta s_\mathrm{D})^{3/2} \sim \delta s_\mathrm{D}$, where $\delta s_\mathrm{D} = s_p - s_s$, we obtain

$$\delta s_\mathrm{D} \sim \varepsilon^{4/5} \,, \qquad \delta\xi_\mathrm{D} \sim \varepsilon^{-1/5} \,. \tag{43}$$

In dimensional units, it means

$$\delta z_\mathrm{D} = \lambda_\mathrm{D}\delta\xi_\mathrm{D} = L\delta s_\mathrm{D} \sim \lambda_\mathrm{D}^{4/5} L^{1/5} \,.$$

The same estimate was found in Refs [52–55]. From this, it is seen that, for $\varepsilon = \lambda_\mathrm{D}/L \to 0$ in the scale given by formula (34), the Debye sheath thickness δs_D turns out to be zero, whereas in the scale given by formula (32), the same, in fact, thickness $\delta\xi_\mathrm{D}$ will be infinite. A poor understanding of this fundamental point is a rich source of sometimes hotly debated paradoxes [28, 56–60].

The electric field at the distance δz_D from the singularity, i.e.

$$E_s \sim \frac{T_\mathrm{e}}{e\lambda_\mathrm{D}^{2/5} L^{3/5}} \,, \tag{44}$$

is small compared to the electric field $E \sim T_\mathrm{e}/e\lambda_\mathrm{D}$ in the Debye sheath, while the potential

$$\varphi_s \sim -\frac{T_\mathrm{e}}{e} \frac{\lambda_\mathrm{D}^{2/5}}{L^{2/5}} \tag{45}$$

is small compared to the potential $\varphi \sim -T_\mathrm{e}/e$ there.

At $q = 1$, although the solution is not expressible in an explicit form, it is also singular for $u \to 1$ in the sense that the derivative $\mathrm{d}\chi/\mathrm{d}s$ becomes infinite, as was the case at $q = 0$. Now, however, the coordinate of the singularity, $s_p = \pi/2 - 1$, is not numerically equal to unity.

At $q = 2$, it proves possible to solve equation (40c) in u and to find the dependence $u(s)$ in an explicit form, but the resulting expression is cumbersome and will not be presented here. We only note that the singularity is located at point $s_p = 1/3$.

Comparing the three panels in Fig. 5a–c, the results of calculations for different ionization models are very similar. In fact, the plots of the potential, ion velocity, plasma density, and current density go almost unchanged with q and differ only by the numerical value of the singularity coordinate s_p. In all three cases considered, as one moves from $u = 0$ (wall) to $u = 1$ (singularity), the plasma density n decreases by a factor of two, whereas the ion flux density increases monotonically from 0 to 1 due to ionization. Ions in the ionization zone are accelerated due to the potential drop from

$$\chi_\mathrm{pl} = \ln 2 = 0.693 \tag{46}$$

to zero, with the plasma density decreasing from $n_\mathrm{pl} = 2n_0$ to n_0. Importantly, in all three examples, the Bohm criterion is satisfied only marginally, i.e., in the equality form

$$v_0 = c_\mathrm{s} \tag{47}$$

(recall that v_0 was defined in Section 2 as the value of v_i at $\varphi = 0$). The order of singularity is also the same for all three cases, so that the estimates of the electric field, formula (44), and potential, formula (45), at the boundary for matching the obtained solutions to the Debye sheath apply to all the examples considered.

We are now in a position to somewhat 'improve' the definition that was given in Section 3 for the loose boundary between the quasineutral plasma and the Debye sheath. Inequalities (18) and (19) assign to this boundary the value of $\chi = 0$. But if we think of this boundary as an imaginary interface between the quasineutral ionization zone and the collisionless charged sheath, it should be admitted that at this boundary $\chi = \chi_s = e\varphi_s/T_\mathrm{e} \sim -(\lambda_\mathrm{D}/L)^{2/5}$. However, the difference between $\chi = 0$ and $\chi = \chi_s$ is important only in calculating the Debye sheath thickness, whereas the difference between their associated electron densities at $\chi = 0$ and $\chi = \chi_s$ is absolutely negligible. The same is true for the ion flow velocity and ion current density. In addition, we will see that χ_s has a different value in the kinetic model of the ionization zone, which is described in Section 8. As a first

approximation then, we can consider that $\chi_s \approx 0$, the same as we did in Section 3.

7. Generalized Bohm's criterion

In Section 2, the Bohm criterion was formulated for the simplest (and not entirely natural) model of cold ions with only two distribution parameters: the ion number density n_i, and flow velocity v_i. For an arbitrary ion distribution function $f(v_z)$, the Bohm criterion can be generalized by writing it down in the form

$$\langle v_z^{-2}\rangle^{-1/2} \geqslant \sqrt{\frac{T_e}{m_i}}, \tag{48}$$

with

$$\langle v_z^{-2}\rangle = \frac{1}{n_i}\int_0^\infty \frac{f(v_z)}{v_z^2}\,\mathrm{d}v_z\,.$$

This criterion was first established by Harrison and Thompson [61], but their derivation was not accepted as convincing. The generalized Bohm criterion has been discussed at various levels of rigor in the literature [11, 30, 35, 42, 62, 63]. Allen [64] mentions the criterion in the form of the equality

$$\langle v_z^{-2}\rangle^{-1/2} = \sqrt{\frac{T_e}{m_i}}. \tag{49}$$

In his remarkable paper [65], Allen highlights the physical meaning of this condition and shows that the generalized Bohm criterion in the form (49) follows from the dispersion relation for ion-sound waves. Featuring a negative frequency $\omega = k(c_s - v_0)$, waves propagate backward against the ion flow, i.e., for $v_0 > c_s$, a perturbation is carried forward by the flow. In this case, the current collector cannot have any effect on the processes in the ion source.

The fact that the Bohm criterion is almost always (except a few artificial models) satisfied in the form of an equality was discussed by Riemann [30]. Of the several arguments Riemann advances in favor of this treatment of the criterion, one, in fact, follows Allen's reasoning [65], which is reproduced in one form or another in Refs [63, 66–71].

The Bohm criterion for a system involving more than one sort of ion has also been discussed [72, 73].

8. Plasma equation

Turning now to the kinetic description, consider a plasma layer between two parallel absorbing walls located at $z = \pm L$. The system is considered to be symmetrical about the middle plane $z = 0$, so that we will restrict ourselves to the region of $z \geqslant 0$. The plasma consists of electrons and one sort of singly charged positive ions. As was the case with Bohm's theory, the electrons are again taken to be Boltzmann-distributed with a fixed temperature T_e. Because ions are due to the ionization of a cold homogeneous background of a neutral gas, they are created with zero velocity and then move exclusively in the direction of the electric field. We will find the ion distribution function $F(z, v_z)$ from the kinetic equation

$$v_z\frac{\partial F}{\partial z} - \frac{e}{m_i}\frac{\mathrm{d}\varphi}{\mathrm{d}z}\frac{\partial F}{\partial v_z} = S_i\delta(v_z)\,, \tag{50}$$

where, as in Sections 5 and 6, S_i denotes the ion source. For convenience, we introduce the dimensionless variables

$$\epsilon = \frac{m_i v_z^2}{2T_e} + \frac{e\varphi}{T_e}\,,\quad \chi = \frac{e\varphi}{T_e}\,,\quad s(\chi) = \frac{z}{L}\,,$$

$$\sigma(\chi) = \frac{LS_i}{n_0 c_s}\,,\quad n = \frac{n_i}{n_0}\,,$$

where, as before, L denotes the characteristic ionization length (to be determined quantitatively later), n_0 is the electron density at $\chi = 0$, and $c_s = \sqrt{T_e/m_i}$ is the ion speed of sound. As the notation $s = s(\chi)$ suggests, we consider the dimensionless potential χ rather than the dimensionless coordinate s as an independent variable. Accordingly, we introduce the dimensionless distribution function

$$f(\epsilon, \chi) = \frac{c_s}{n_0}\,F(z, v_z) \tag{51}$$

as a function of the dimensionless energy ϵ and dimensionless potential χ. In this notation, kinetic equation (50) becomes

$$\frac{\partial f}{\partial \chi} = \sigma(\chi)\,s'(\chi)\,\delta(\epsilon - \chi)\,, \tag{52}$$

where the quantity $s' = \mathrm{d}s/\mathrm{d}\chi$ is the inverse of the electric field strength. In integrating equation (52), we shall assume that the potential $\chi(s)$ is a monotonically decreasing function similar to that shown by the dashed line in Fig. 5, so that at a given energy ϵ the argument of the delta function $\delta(\epsilon - \chi)$ on the right-hand side cannot be zero at more than one point. Because the right-hand side of equation (52) is zero everywhere except at $\chi = \epsilon$, the distribution function $f(\epsilon, \chi)$ is, in fact, independent of its second argument except for this point, where the function $f(\epsilon)$ possesses a discontinuity. Hence, one has

$$f(\epsilon, \chi) = \begin{cases} f_-(\epsilon) & \text{for } \chi < \epsilon\,, \\ f_+(\epsilon) & \text{for } \chi > \epsilon \end{cases} \tag{53}$$

and

$$f_+(\chi) - f_-(\chi) = \sigma(\chi)\,s'(\chi)\,.$$

In a monotonically decreasing potential $\chi(s)$, the point with a potential χ is inaccessible to ions with energy $\epsilon < \chi$. Hence, one arrives at

$$f_+(\epsilon) = 0\,,\quad f_-(\epsilon) = -\sigma(\epsilon)\,s'(\epsilon)\,, \tag{54}$$

where $s' < 0$. In this case, the ion number density is given by

$$n = \int_\chi^{\chi_{pl}} \frac{f_-(\epsilon)}{\sqrt{2(\epsilon - \chi)}}\,\mathrm{d}\epsilon = -\int_\chi^{\chi_{pl}} \frac{\sigma(\epsilon)\,s'(\epsilon)}{\sqrt{2(\epsilon - \chi)}}\,\mathrm{d}\epsilon\,, \tag{55}$$

where χ_{pl} is the maximum value of the potential in the plasma (equal as well to the potential of the quasineutral plasma outside of the region where ionization sources are at work). Because in dimensionless variables the electron density assumes the form $\exp(\chi)$, Poisson's equation for the self-consistent potential χ takes the form

$$\varepsilon^2\,\frac{\mathrm{d}^2\chi}{\mathrm{d}s^2} = \exp(\chi) - n = \exp(\chi) + \int_\chi^{\chi_{pl}} \frac{\sigma(\epsilon)\,s'(\epsilon)}{\sqrt{2(\epsilon - \chi)}}\,\mathrm{d}\epsilon\,. \tag{56}$$

The dimensionless ionization rate, $\sigma = LS_\mathrm{i}/n_0 c_\mathrm{s}$, is defined in terms of two variables: the ionization zone thickness L, and the electron number density n_0 at the location where $\chi = 0$, both as yet unknown. Assuming, as in Section 6, that $S_\mathrm{i} = S_q n_\mathrm{e}^q$ and $L = n_0 c_\mathrm{s}/S_q n_0^q$, we have

$$\sigma(\chi) = \exp(q\chi) \tag{57}$$

for ionization models with different values of parameter q. Thus, the final definition of L and n_0 is postponed until the coordinate s_p of the Debye sheath is calculated.

In the plasma approximation, the term with ε^2 in Poisson equation (56) is omitted, yielding the 'plasma equation', which is, essentially, the quasineutrality condition

$$\int_\chi^{\chi_\mathrm{pl}} \frac{\sigma(\epsilon)\, s'(\epsilon)}{\sqrt{2(\epsilon-\chi)}}\,\mathrm{d}\epsilon = -\exp(\chi)\,. \tag{58}$$

The plasma equation, which is recognized as the first order Volterra integral equation, was first derived and studied numerically by Tonks and Langmuir [19]. In Harrison and Thompson's paper [61], it is solved by the Abel transform to give

$$\sigma(\chi)\, s'(\chi) = \frac{\sqrt{2}}{\pi}\frac{\mathrm{d}}{\mathrm{d}\chi}\int_\chi^{\chi_\mathrm{pl}} \frac{\exp(\eta)}{\sqrt{\eta-\chi}}\,\mathrm{d}\eta\,, \tag{59}$$

which, when integrated, becomes

$$\sigma(\chi)\, s'(\chi) = -\frac{\sqrt{2}}{\pi}\left[\frac{\exp(\chi_\mathrm{pl})}{\sqrt{\chi_\mathrm{pl}-\chi}} - \sqrt{\pi}\,\exp(\chi)\,\mathrm{erfi}\left(\sqrt{\chi_\mathrm{pl}-\chi}\right)\right], \tag{60}$$

where

$$\mathrm{erfi}(x) = \frac{2}{\sqrt{\pi}}\int_0^x \exp(t^2)\,\mathrm{d}t\,,$$

and the ionization rate $\sigma(\chi)$ is determined in equation (57). It is interesting that ion distribution function

$$f(\epsilon,\chi) = \begin{cases} \dfrac{\sqrt{2}}{\pi}\left[\dfrac{\exp(\chi_\mathrm{pl})}{\sqrt{\chi_\mathrm{pl}-\epsilon}} - \sqrt{\pi}\exp(\epsilon)\,\mathrm{erfi}\left(\sqrt{\chi_\mathrm{pl}-\epsilon}\right)\right], & \chi < \epsilon < \chi_\mathrm{pl} \\ 0, & \epsilon < \chi \quad \text{or} \quad \chi_\mathrm{pl} < \epsilon \end{cases} \tag{61}$$

does not depend on $\sigma(\chi)$.

According to Eqn (60), the derivative $s'(\chi)$ starts from a singularity for $\chi \to \chi_\mathrm{pl}$, then monotonically decreases (in absolute value) for $\chi < \chi_\mathrm{pl}$ and becomes zero at $\chi = \chi_\mathrm{pl} - 0.854$. At the point of singularity at $\chi = \chi_\mathrm{pl}$, the electric field vanishes, so the potential $\chi(s)$ has a maximum there, whereas the zero of the derivative $s'(\chi)$ represents a singularity in an electric field, which, as we saw in Section 6, corresponds to the Debye sheath. The root of the equation $s'(\chi) = 0$ does not depend on the shape of the function $\sigma(\chi)$ and is therefore universal for all ionization models. Following the convention adopted in Section 6, let us agree again that the potential at the entrance to the Debye sheath is close to zero. Then, the root of an equation $s'(0) = 0$ gives the value of the potential maximum:

$$\chi_\mathrm{pl} = 0.854\,. \tag{62}$$

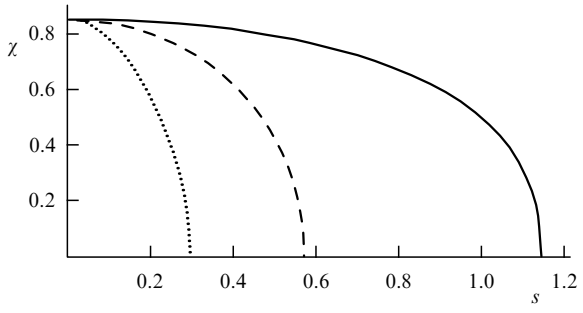

Figure 6. Ionization zone potential profile in the kinetic model of a 'plasma equation' at $q = 0$ (solid line), $q = 1$ (dashed line), and $q = 2$ (dotted line).

The plasma density at the maximum, $n_\mathrm{pl} = \exp(\chi_\mathrm{pl})\, n_0$, is a factor of 2.349 larger than the density n_0 at the entrance to the Debye sheath. Note that quantity (62) is 23% larger than the similar-in-meaning value (46) written down in Section 6. Moreover, it is larger than $\chi_\mathrm{pl} = 1/2$, a value which is most often used when calculating the density drop over the Debye presheath [11–13, 24, 74].

We will further assume that the potential maximum resides in the center of the plasma at $s = 0$. Figure 6 plots the potential profiles calculated by integrating equation (60) for three values of parameter q. The result of the integration can be expressed implicitly as

$$s(\chi) = \sqrt{\frac{2}{\pi}}\exp(\chi)\,\mathrm{erfi}\left(\sqrt{\chi_\mathrm{pl}-\chi}\right)$$

at $q = 0$, as

$$s(\chi) = \sqrt{\frac{2}{\pi}}\left[\left(\frac{1}{2}+\chi-\chi_\mathrm{pl}\right)\mathrm{erfi}\left(\sqrt{\chi_\mathrm{pl}-\chi}\right) + \frac{1}{\sqrt{\pi}}\exp(\chi_\mathrm{pl}-\chi)\sqrt{\chi_\mathrm{pl}-\chi}\right]$$

at $q = 1$, and as

$$s(\chi) = \frac{\sqrt{2/\pi}}{q-1}\left[\sqrt{q}\,\exp\left[-(q-1)\,\chi_\mathrm{pl}\right]\mathrm{erfi}\left(\sqrt{q(\chi_\mathrm{pl}-\chi)}\right) - \exp\left[-(q-1)\,\chi\right]\mathrm{erfi}\left(\sqrt{\chi_\mathrm{pl}-\chi}\right)\right]$$

in the general case. Close to the singularity, the potential takes the form

$$\chi = \frac{\sqrt{s_p - s}}{0.579}\,, \tag{63}$$

where $s_p = 1.144$ at $q = 0$, $s_p = 0.572$ at $q = 1$, and $s_p = 0.296$ at $q = 2$. A comparison with calculated results of Section 6 reveals that the kinetic and hydrodynamic models place the singularity at about the same coordinate s_p.

In addition to the already mentioned Refs [19, 61], the solution of the plasma equation (56) was examined in Refs [4, 30, 32, 33, 75].

Returning to Poisson's equation (56) smooths out the singularity for $\chi \to 0$, resulting in the derivative $s'(\chi)$ vanishing nowhere (and the electric field goes to infinity nowhere). Because the approximate expression (63) implies that $s'(\chi) \sim -\chi$ for $\chi \to 0$, it follows that a deviation from

such a dependence results in the difference $\exp(\chi) - n$ on the right-hand side of the equation, for $\chi \to 0$, being of order $\chi^{3/2}$ rather than zero. Therefore, the quasineutrality approximation becomes inadequate where

$$\varepsilon^2 \frac{\mathrm{d}^2\chi}{\mathrm{d}s^2} \sim \chi^{3/2} .$$

From this expression, substituting formula (63), it is straightforward to estimate the Debye sheath thickness and then also the potential at the point where the quasineutral solution is matched with the exact solution:

$$\delta s_\mathrm{D} = s_p - s_s \sim \varepsilon^{8/9} , \quad \delta\xi_\mathrm{D} = \xi_p - \xi_s \sim \varepsilon^{-1/9} , \quad \chi_s \sim \varepsilon^{4/9} .$$

Here, as in Section 6, the subscript s labels quantities referring to the matching point. In dimensional units, one finds

$$\delta z_\mathrm{D} \sim \lambda_\mathrm{D}^{8/9} L^{1/9} , \ \varphi_s \sim -\frac{T_\mathrm{e}\lambda_\mathrm{D}^{4/9}}{eL^{4/9}} , \ E_s \sim \frac{T_\mathrm{e}}{e\lambda_\mathrm{D}^{4/9} L^{5/9}} , \quad (64)$$

which differs somewhat from the analogous quantities (43)–(45) calculated in the hydrodynamic approximation.

References [32, 76] provide a more detailed study of the region between the ionization zone and Debye sheath.

To describe the Debye sheath quantitatively requires that the problem be reformulated in terms of the Debye scale by replacing $s = z/L$ with $\xi = z/\lambda_\mathrm{D} = s/\varepsilon$. On this scale, the Poisson equation

$$\frac{\mathrm{d}^2\chi}{\mathrm{d}\xi^2} = \exp(\chi) - n \quad (65)$$

does not contain the small parameter ε, so the space charge cannot be neglected. On the other hand, because the Debye sheath is collisionless, the ion distribution function within it (for $\chi < 0$) is known in the form of the limit $f(\epsilon, 0)$ of the distribution function (61) at the edge of the quasineutral plasma (for $\chi \to 0$), with $f(\epsilon, 0) = 0$ for $\epsilon < 0$. Thus, the ion density in the Debye sheath is given by

$$n(\chi) = -\int_0^{\chi_\mathrm{pl}} \frac{\sigma(\epsilon)\, s'(\epsilon)}{\sqrt{2(\epsilon - \chi)}}\, \mathrm{d}\epsilon = \exp(\chi) - \int_0^{\chi} \frac{\sigma(\epsilon)\, s'(\epsilon)}{\sqrt{2(\epsilon - \chi)}}\, \mathrm{d}\epsilon . \quad (66)$$

Substituting Eqn (66) into Eqn (65) gives in the limit of $\chi \to 0$:

$$\frac{\mathrm{d}^2\chi}{\mathrm{d}\xi^2} = -0.947(-\chi)^{3/2} ,$$

from which we have the asymptotic form

$$\chi = -\left(\frac{4.59}{\xi_p - \xi}\right)^4 \quad (67)$$

for $\xi \to -\infty$, which differs qualitatively from the hydrodynamic asymptotic form (12).

Substituting the distribution function $f(\epsilon, 0)$ into the generalized Bohm criterion (48) yields the condition

$$\int_0^{\chi_\mathrm{pl}} \frac{\sigma(\eta)\left|s'(\eta)\right|}{\left[2(\chi - \eta)\right]^{3/2}}\, \mathrm{d}\eta \leqslant 1 . \quad (68)$$

It can be shown that this condition is satisfied in the form of an equality [30, 61]. Importantly, the ion flow velocity at the entrance to the Debye sheath exceeds somewhat the ion speed of sound:

$$v_0 = \int v_z F\, \mathrm{d}v_z = c_\mathrm{s} \int_0^{\chi_\mathrm{pl}} \sigma(\eta)\left|s'(\eta)\right| \mathrm{d}\eta = 1.144 c_\mathrm{s} . \quad (69)$$

This is possibly due to the fact that, as indicated above, the potential drop in the ionization zone is 23% larger than predicted by Bohm's theory.

9. Localized ion source

Let us remove the assumption that ions emerge with a zero initial velocity. Of interest is the exactly solvable example (Cohen and Ryutov [35]) of a spatially localized ion source which injects *finite*-velocity ions into the plasma, a situation which approximately corresponds to how the users of the PBGUNS [77] and POISSON-2 [78, 79] codes should specify the ion source and which, in a sense, invalidates the statement that the Bohm criterion is most without exception satisfied in the form of the equality $v_0 = c_\mathrm{s}$. Cohen's and Ryutov's example involves the formation of a supersonic ($v_0 > c_\mathrm{s}$) ion flow but assumes, in a less than natural way, that the size of the ionization zone is less than the Debye length, $L < \lambda_\mathrm{D}$ — contrary to the assumption $L \gg \lambda_\mathrm{D}$ we have always used.

Cohen and Ryutov considered a one-dimensional plasma sandwiched between two flat ion collectors. The localized ion source, which resided in the symmetry plane of the problem, $z = 0$, midway between absorbing walls, injected ions with a finite initial velocity v_in to either side symmetrically. Due to the symmetry, the electric field in the plane $z = 0$ should be zero: $E(0) = 0$.

If the initial ion velocity v_in was equal to the speed of sound c_s, then the potential $\varphi_\mathrm{in} = \varphi(0)$ in the injection plane settled to the level of the quasineutral plasma potential $\varphi_s \approx 0$ at the entrance to the Debye sheath, so the ion velocity v_0 in the quasineutral region of the plasma was also c_s, and the Bohm criterion was satisfied in the form of the equality $v_0 = c_\mathrm{s}$. For $v_\mathrm{in} < c_\mathrm{s}$, the potential φ_in at the injection point was found to be larger than φ_s, and close to the source a Debye sheath formed, where ions were accelerated to beyond the speed of sound: $v_0 > c_\mathrm{s}$. In the limit of $v_\mathrm{in} \to 0$, the ion velocity in the quasineutral part of the plasma approaches $v_0 = 1.585\, c_\mathrm{s}$, a value which Dubinov and Senilov [80] declared to be the maximum ion outflow velocity from a plasma emitter. We will show, however, that solutions exist with a flow velocity $v_0 > 1.585\, c_\mathrm{s}$, although they are inconsistent with the boundary condition $E(0) = 0$.

Proceeding to calculations, let us consider a plasma layer between two parallel absorbing walls, assuming the presence of an ion source given by

$$S_\mathrm{i}(z, v_z) = S_0 \delta(z)\left[\delta(v_z - v_\mathrm{in}) + \delta(v_z + v_\mathrm{in})\right] . \quad (70)$$

It is assumed that the function $S_\mathrm{i}(z, v_z)$ is even in both its arguments and falls off sufficiently rapidly away from the source region for the z dependence to be represented by a delta function, as in formula (70). The initial ion velocity v_in is generally different from zero. As we will see, the potential $\varphi(z)$ has a maximum $\varphi_\mathrm{in} = \varphi(0)$ at the ion injection point; therefore, there are no ion stopping points close to the source, i.e., $m_\mathrm{i} v_\mathrm{in}^2/2 + e\varphi_\mathrm{in} > e\varphi(z)$ for all $z > 0$. Hence, the ion

velocity

$$v_z = \sqrt{v_{\rm in}^2 + \frac{2e}{m_{\rm i}}\left[\varphi_{\rm in} - \varphi(z)\right]} \tag{71}$$

vanishes nowhere, and the ion number density

$$n_{\rm i} = \frac{S_0}{v_z} \tag{72}$$

nowhere becomes infinite. As regards the electron density $n_{\rm e}$, we will again assume that it obeys the Boltzmann distribution (2). Because the electric potential is defined to within a constant, this constant can be chosen such that $n_{\rm i} = n_{\rm e}$ at $\varphi = 0$. Then, it is straightforward to show that

$$n_0 = \frac{S_0}{\sqrt{v_{\rm in}^2 + 2e\varphi_{\rm in}/m_{\rm i}}} \tag{73}$$

is the electron density in that part of the quasineutral region where $\varphi = 0$.

Introducing the dimensionless quantities

$$\chi = \frac{e\varphi}{T_{\rm e}}\,, \quad \xi = \frac{z}{\lambda_{\rm D}}\,, \quad u_0^2 = \frac{m_{\rm i}v_{\rm in}^2 + 2e\varphi_{\rm in}}{T_{\rm e}}\,,$$

where, as before, $\lambda_{\rm D} = \sqrt{T_{\rm e}/4\pi e^2 n_0}$, Poisson equation (1e) yields equation (6) for the dimensionless potential χ, which allows the useful mechanical analogy we already used in Section 2. According to formula (8), this equation has the energy integral

$$W = \frac{1}{2}\left(\frac{\partial\chi}{\partial\xi}\right)^2 + U(\chi)$$

and describes the motion of an imaginary pseudoparticle in the effective potential $U(\chi)$ specified by formula (7) provided that χ and ξ are interpreted as a coordinate and time in a certain mechanical system.

The effective potential $U(\chi)$ at $\chi = 0$ has either a minimum if $u_0^2 < 1$ or a maximum if $u_0^2 > 1$, as shown in Fig. 7; therefore, the point $\chi = 0$ is stationary for a pseudoparticle with zero energy, $W = 0$.

Let us consider the motion of a pseudoparticle with energy $W \to 0+$ (i.e., $W \to 0$ for $W > 0$).

In the case of $u_0^2 < 1$ (Fig. 7a), such a pseudoparticle is locked in the neighborhood of the effective energy minimum near $\chi = 0$, so there is no solution which links the quasineutral region $\chi \approx 0$ to the unipolar sheath $\chi \lesssim -4$.

The situation changes if $u_0^2 > 1$. In this case, the region $\chi < 0$ becomes accessible in full to a pseudoparticle with $W \to 0+$. It is readily seen that the 'time' it takes for such a pseudoparticle to reach the absorbing wall (ion collector) somewhere in the region $\chi \to -\infty$ will be very long, because the pseudoparticle almost stops near the maximum of the effective potential at $\chi = 0$ and stays there very long before it is accelerated and continues to move toward the wall. In a real-life system, some part of the trajectory of such a pseudoparticle corresponds to a long quasineutral zone located between the ion source and the Debye sheath and where the variation of the electric potential is very slow.

When analyzing the solution of the Poisson equation in Section 2, we in fact assumed that the pseudoparticle starts from a certain point $\chi \to 0-$ with a small 'velocity' $d\chi/d\xi \to 0-$. In this section, we will continue this solution into the region of $\chi > 0$ and will see a second Debye sheath forming there near the source, in which the injected ions are preliminarily accelerated.

Importantly, the function $U(\chi)$ for $\chi = \chi_{\rm in} > 0$ has a second zero if

$$1 < u_0^2 < 2.513\,, \tag{74}$$

as shown in Fig. 7b. The upper boundary of interval (74) is determined from the equation $U(u_0^2/2) = 0$ (see below). The trajectory of a pseudoparticle which starts with zero 'velocity' $d\chi/d\xi = 0$ from a point close to $\chi = \chi_{\rm in}$ satisfies the boundary condition $E(0) = 0$ at the ion source due to the symmetry of the problem with respect to the $z = 0$ plane. On the other hand, for such a trajectory $W \to 0$, so that it 'slows down' near $\chi = 0$ to form a long quasineutral zone going over to a Debye sheath, as shown in Figs 8a, b by a solid line. The dimensionless local ion velocity

$$u = \frac{v_{\rm i}}{c_{\rm s}} = \sqrt{u_0^2 - 2\chi}$$

is shown in Fig. 8 by a dashed line. In Figs 8a, b, its initial value

$$u_{\rm in} = \sqrt{u_0^2 - 2\chi_{\rm in}}$$

at the injection point is greater than zero. However, it tends to zero as $u_0^2 \to 2.513$. On the contrary, $\chi_{\rm in} \to 0$ and, hence, $u_{\rm in} \to u_0 \to 1$ as $u_0^2 \to 1$. As seen from Figs 8a, b, the injected ions are accelerated to a supersonic velocity during the time they move through the Debye sheath in the zone of preliminary acceleration near the ion source, where $\chi > 0$. The acquired velocity remains nearly constant, as ions move through the quasineutral plasma, where $\chi \approx 0$. The ions then start to be accelerated again in the second Debye sheath, where $\chi < 0$.

In the case of $u_0^2 > 2.513$ (Fig. 7c), the second zero of the effective potential $\chi = \chi_{\rm in} > 0$ disappears, because the func-

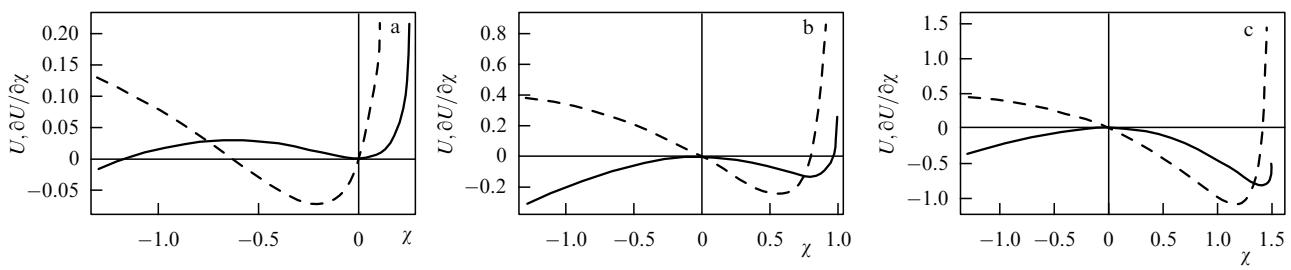

Figure 7. Plots of the effective potential $U(\chi)$ (solid line) and its derivative $\partial U(\chi)/\partial\chi$ (dashed line): (a) $u_0^2 = 1/2$, (b) $u_0^2 = 2$, and (c) $u_0^2 = 3$.

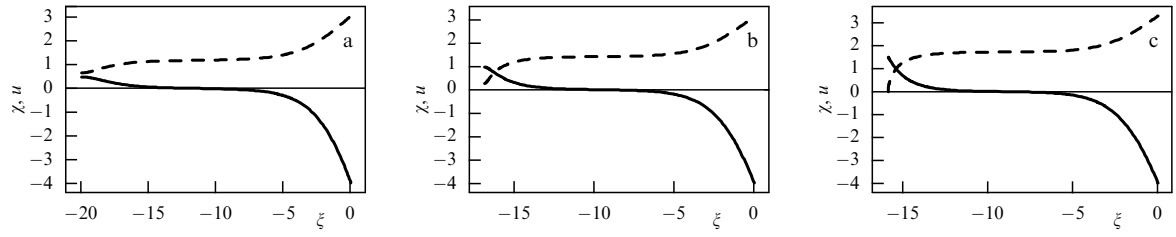

Figure 8. Potential $\chi(\xi)$ (solid line) and local velocity u (dashed line) profiles for $W = 0.5 \times 10^{-4}$: (a) $u_0^2 = 1.4$; (b) $u_0^2 = 2.0$, and (c) $u_0^2 = 3.0$. Peak in χ on the left — the Debye preacceleration sheath close to the localized ion source; the well in χ on the right — the Debye sheath going over to the unipolar sheath; a plateau between — a quasineutral zone, which becomes very long for $W \to 0$.

tion $U(\chi)$ becomes complex-valued for $\chi > u_0^2/2$. As a result, it turns out that we cannot satisfy the boundary condition $d\chi/d\xi = 0$ corresponding to the vanishing of the electric field $E(0)$ in the symmetry plane.

Abandoning the condition $E(0) = 0$ (either by removing the symmetry requirement or by allowing for the electric field discontinuity on either side of the $z = 0$ plane) makes the point $U = 0$ undistinguishable from other points. We can then place the source at any point in the range of existence of the solution $\chi < u_0^2/2$, where $U \leqslant 0$ (Figs 8b, c). The value of $\chi = u_0^2/2$ at the injection point will then correspond to a zero initial ion velocity, $u_{in} = 0$.

In the PBGUNS code mentioned above, the imaginary ion source is placed on the rear wall of the plasma emitter chamber. The ions are liberated from this wall with a specified initial velocity. To our knowledge, the electric field is not assumed to be zero there, so that the corresponding potential distribution can be described by that part of the solid line in Fig. 8 which starts from any of its points located to the left of the quasineutral zone, provided the ion velocities are initially subsonic. In the quasineutral zone, the flow is supersonic, and the electric field is near zero. Hence, a solution which starts from any point in the quasineutral zone describes a supersonic ion source in which a Debye preacceleration sheath is absent. For such a source we should set $\varphi_{in} = 0$ in formula (73). In real-life devices, arc sources are used to inject supersonic ions into the plasma [81].

10. Emission current

Within the Debye sheath, where both ionization and Coulomb collisions are of negligible importance due to the sheath's small thickness, the ion current density is a constant quantity

$$j_p = en_i v_i = en_0 v_0 \,, \tag{75}$$

to which we will refer as the '*emission current*'. Bohm's criterion (17) bounds the emission current from below:

$$j_p \geqslant en_0 c_s \,. \tag{76}$$

The question now is raised: Is the emission current bounded from above?

In their recent paper [80], Dubinov and Senilov argued that yes, it is and, as shown in Ref. [82], there is formal reasoning behind their claim. Similarly to the procedure followed in Section 9, Dubinov and Senilov consider the motion of a pseudoparticle in an effective potential $U(\chi)$ for $W \to 0+$ by analyzing its trajectory, which starts near the maximum of $U(\chi)$ at $\chi = 0$ with a small positive velocity $d\chi/d\xi > 0$. This trajectory first moves in a reverse direction from the ion collector, reflects near $\chi = \chi_{in} > 0$, and only then starts moving toward the collector for $\chi \to -\infty$. Because, as we saw in Section 9, the reflection point $\chi = \chi_{in}$ disappears for $u_0^2 > 2.513$, such a trajectory exists only in interval (74). From this, Dubinov and Senilov conclude that the ion flow velocity $v_0 = u_0 c_s$ can fall in a relatively narrow range

$$c_s < v_0 < 1.585\, c_s \,, \tag{77}$$

although they fail to explain why the Langmuir sheath in the region $\chi < 0$ should in any way depend on whether a reflection point does or does not exist in the region $\chi > 0$.

If formulated realistically, the problem of the plasma emitter [2] should involve an ion source in the bulk of the plasma. As shown in Section 9, if ions are created with a small velocity, then a Debye sheath forms near the source, in which the electric field accelerates ions to the velocity determined by the Bohm criterion. It is this sheath for which the corresponding part of the pseudoparticle trajectory is between $\chi = \chi_{in}$ and $\chi = 0$. On the other hand, a discussion in the same section shows that suitable solutions exist even for $u_0^2 > 2.513$ if one assumes the presence of sources from which a highly supersonic ion flux is injected into the plasma with the rate significantly exceeding the ion speed of sound. Such sources should apparently be more than one-dimensional, because in one-dimensional volume-ionized systems the Bohm criterion is satisfied in the form of an equality, so that the ion outflow velocity automatically settles to or near the speed of sound. As shown in Section 6, $v_0 = c_s$ in the hydrodynamic approximation and, hence

$$j_p = en_0 c_s \,, \tag{78}$$

whereas the kinetic theory described in Section 8 predicts

$$j_p = 1.144\, en_0 c_s \,. \tag{79}$$

The main conclusion to draw from these theories is that the emission current density is completely determined by bulk plasma processes. As pointed out in monograph [2], this is what makes the fundamental difference between a plasma emitter and thermal emission from the surface of a solid electrode. In a thermionic diode, the external potential controls the emission current density through a mechanism which uses spatial charge to restrict the emission. In the case of a plasma emitter, the emission current is specified; there-

fore, the external potential controls the size of the diode gap, and the plasma occupies exactly that section of the gap necessary to ensure that the emission current is equal to the current predicted by the Child–Langmuir law.

Some authors (see, for example, Refs [11–13, 24, 74]) append a factor of $\exp(-1/2) \approx 0.61$ into the emission current expression (78) and take n_0 to mean the plasma concentration $n_{\rm pl}$ in the region where the ion flow velocity is zero, whereas in formulas (78) and (79), n_0 is the plasma concentration at the entrance into the Debye sheath, where the ion velocity is equal to $c_{\rm s}$. Treating the emission current in this way is not entirely self-consistent, because the emission current is then expressed in terms of quantities that refer to different parts of the plasma. On the other hand, this approach is quite natural if the presheath thickness is much less than the linear size of the plasma, as is the case in the probe measurements of plasma parameters.

The use of probes requires that the plasma temperature and density be relatively low; otherwise, the probes burn out. At a temperature $T_{\rm e} = 1$ eV and density $n = 10^{12}$ cm^{-3}, the mean free path is a mere 1 cm, and the presheath thickness is a few centimeters. If the thickness is smaller than the linear size of the plasma, then it is better to express j_p in terms of the outside-the-sheath plasma density $n_{\rm pl}$ rather than the density n_0 at the 'entrance' into the Debye sheath. Assuming, as in Section 3, that the potential drop over the presheath is 1/2 (in units of $T_{\rm e}/e$) yields $n_{\rm pl} = n_0 \exp(1/2) = 1.649\, n_0$ and formula (78) is equivalent to

$$j_p = 0.607\, e n_{\rm pl} c_{\rm s}\,. \tag{80}$$

However, the hydrodynamic model described in Section 6 predicts the potential drop over the presheath to be $\ln 2 = 0.693$, and $n_{\rm pl} = 2n_0$. We then have

$$j_p = 0.5\, e n_{\rm pl} c_{\rm s}\,. \tag{81}$$

In the kinetic model constructed in Section 8, one has $n_{\rm pl} = n_0 \exp(0.854) = 2.349\, n_0$, and formula (79) is equivalent to

$$j_p = 0.487\, e n_{\rm pl} c_{\rm s}\,, \tag{82}$$

which is identical to Eqn (3.69) in monograph [4] by Forrester. As noted earlier in Ref. [39], formulas (81) and (82) give close results, whereas Eqn (80) obtained heuristically from Eqn (78) is apparently not quite accurate.

11. Numerical simulation of the plasma emitter

Real-life ion sources with a plasma emitter take advantage of arc, RF, or surface-plasma discharges to produce plasma (see, for example, Refs [83–94]). The calculation of such sources in two or three dimensions requires the use of numerical codes. Numerically calculating plasma emitter sources turns out to be much more challenging than in the case of their solid counterparts, the main reason being that the shape of the plasma boundary is not specified beforehand. In multi-aperture systems, the plasma is in contact with a multihole metal grid. If the hole diameters are much larger than the Debye length, then we are dealing with the emission of charged particles from *a free plasma surface*, and the surface itself is referred to as *a plasma meniscus* [13, 74, 95–98]. The shape and location of the meniscus depend on how the plasma is produced, the plasma potential and density, the velocity distribution of plasma particles, and the shape of the focusing electrodes. To further complicate things, there are several sorts of charged particles and of neutral gas, necessitating the introduction of new concepts such as quasineutrality, the Debye length, the mean free path, and the ionization cross section.

In high-current charged particle sources, the Debye length is often too small compared to the device size for numerical codes to resolve it given a reasonable difference grid spacing. Such devices are calculated either by making the grid denser near the meniscus or by using a sharp boundary plasma model. In the latter case, the real potential distribution in the Debye sheath is replaced by model boundary conditions on the free surface of the plasma, the plasma being considered quasineutral up to this surface. The outer surface of the sharp boundary plasma is bordered by a unipolar sheath without there being a Debye sheath between. The one-dimensional theory outlined in the previous sections is intended to provide a correct formulation of the boundary conditions for such numerical codes. The shape of the plasma meniscus and the corresponding free surface boundary conditions are discussed in Section 12. Here, we will briefly review the computer codes for modeling ion sources with a plasma emitter.

Due to the complexity of the problem, such codes are considerably fewer than those for other problems in electronic optics. There are three basic modules in any available code: (1) solving Maxwell's equations for electric and magnetic fields or the Poisson equation for the electric potential; (2) solving the kinetic equation for the distribution function of charged plasma particles or their hydrodynamic analogs, and (3) carrying out an iterative procedure to match these solutions.

The numerical methods for solving kinetic and hydrodynamic equations include the method of macroparticles, a range of difference schemes [99], the method of integral equations [100], the finite element method [101], and combinations thereof. The often-used way to model plasma and beams in nonstationary problems is to apply the 'particles-in-cells' (PIC or CIC) method [102]. Stationary problems are treated by the trajectory method or by the method of tube currents [99], the choice depending on the nature of the problem at hand.

Whealton and coworkers list in paper [103] the plasma emitter modeling codes that were developed at the early stages of computer technology and are designed for analyzing the sources of negative ion beams and discuss some aspects of emitter modeling in two and three dimensions. A brief discussion of numerical codes currently under active development will now be given.

11.1 PBGUNS

The interactive code PBGUNS (Particle Beam GUN Simulations) [77, 104, 105], which has been developed since 1960 as a means to model first electron and then ion beams, is a 2.5-dimensional (2.5D) code (i.e., two-dimensional in coordinate space and three-dimensional in velocity space) and calculates all three magnetic field components. The electrons of the emitting plasma are modelled by a Boltzmann density distribution, and ions by the method of tube currents, the tubes starting from the inner surface of the plasma chamber, where the current density and ion velocity are specified by the user. The recommended value of the initial ion energy corresponds to the electron temperature. The volumetric

charge density of the emitted ion flux is obtained from the equation of continuity for tube currents on a square grid, which becomes denser near the free surface of the plasma. The electric potential distribution is calculated iteratively using the method of relaxation for square grid difference schemes. PBGUNS calculates the shape of the plasma meniscus and does not require that the meniscus curvature or any other beam or plasma parameters be known to the user; what it does require, though, is the user's knowledge of the meniscus's initial location and shape.

PBGUNS treats a wide range of problems concerning the formation and transport of relativistic and nonrelativistic beams of electrons and of (positive and negative) ions in systems involving plasma and solid emitters, contains a convenient interactive interface for the input and output of information, and features a vast archive of sample tasks. Among its weaknesses is performance instability, probably due to the statistically small number of trajectories and due to the fact that the source operates in regimes close to physically unstable states. Furthermore, the code is designed to handle only one plasma region, preventing modeling of counter-propagating electron and ion beams emitted from more than one plasma region simultaneously.

11.2 COBRA-3

The three-dimensional code COBRA-3 [106–108] was developed to model the formation of high-current ion beams in systems with a plasma emitter in self-consistent electric and magnetic fields. The Poisson equation in the difference form is solved by the iterative method of upper relaxation; the equations of motion of ions are integrated, including the contribution of ions to the space charge. COBRA-3 assumes the Boltzmann electron distribution and calculates the free surface shape of a plasma which emits differently charged ions. The parameters of the emitted ions are determined from an experimental database. If need be, the self-magnetic field of the currents involved can be taken into consideration [109]. The predecessor of COBRA-3 was the AXCELL code [110–112].

11.3 POISSON-2

The applied software package POISSON-2 [78, 79, 113–118] is designed for solving 2.5-dimensional (plane and axisymmetric) stationary problems in the electron and ion optics of high-current relativistic sources. POISSON-2 is capable of handling sources with particles of ten kinds emitted by several surfaces simultaneously. Algorithms for modeling plasma emitters in POISSON-2 have been developed since the early 1980s with consideration for collisional, ionization, charge exchange, and other processes in gas-filled accelerators [114, 115].

The development of this software package was given an impetus by 2006 experiments on the generation in plasma emitter accelerators of high-power long-duration pulses for heating plasma in open systems for magnetic plasma confinement [116]. Currently, the package is capable of simulating the simultaneous generation of an electron beam and an ion beam emitted counter to each other from the cathode and anode plasma surfaces, respectively, the beam and emission-surface shapes being calculated by iteratively matching the fields and current tubes [78].

Figure 9 illustrates the calculation of an axisymmetric elementary cell of a multiaperture electron source; the electrons injected into the plasma of the open plasma trap

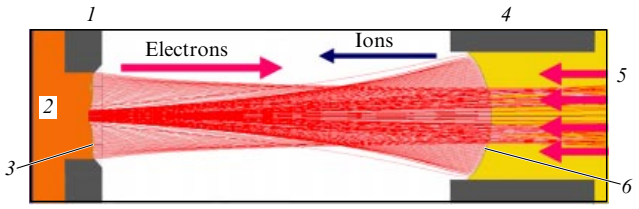

Figure 9. Example of modeling the cell of a multiaperture electron beam source using the POISSON-2 package. Beam electrons penetrating into the plasma behind the anode cause it to heat and expand toward the cathode: *1*, cathode; *2*, plasma; *3*, cathode plasma boundary; *4*, anode; *5*, plasma flux from the magnetic trap; *6*, anode plasma boundary. Diode voltage $U = 100$ kV, accelerating gap $d = 12$ mm, electron and ion current densities are 60 A cm^{-2} and 1 A cm^{-2}, respectively, and the directed ion energy is 7 keV.

located behind the anode heat the plasma and thereby cause it to expand and to flow out with a large directed velocity into the accelerating gap.

The two-dimensional Poisson equation is solved by the method of integral equations, and the flow of particles is calculated by the current tube method, the current tubes featuring a central trajectory and a variable cross section. Relativistic equations of motion are solved by the Boris method [119]. The space charge density is calculated for the cell centers of a rectangular nonuniform grid in solving the continuity equation. The potentials and electric fields are calculated at the grid nodes and interpolated to the particle coordinates. The magnetic field is determined as the sum of the specified external field and the self-magnetic field of the current tubes.

Because the Debye length is assumed to be infinitesimal, POISSON-2 leans upon a sharp-boundary plasma model. The electric field at the boundary is finite and is determined by substituting the plasma parameters into formulas which are similar to Eqns (9), (28) but differ from them in including the space charge of the particles in the counter flow, as shown in Fig. 9. Field and current trajectory matching are performed iteratively through the space charge relaxation mechanism. An improvement in the calculated location and shape of the free plasma surface was carried out in another iteration procedure which uses the displacement of the surface nodes along one of the coordinates. The iteration process terminates when the emission current density determined by the plasma parameters is equal to the current the Child–Langmuir law predicts for the accelerating gap. A more detailed description of the algorithm for the plasma meniscus shape is given in Section 12.

11.4 ELIS

Also noteworthy among the codes for plasma emission electronics is the ELIS software design developed by the V A Gruzdev team [120–122] in Belarus. ELIS's application is limited to two types of source geometry: a hollow cathode with an emission hole, and a hollow cathode coated with an emission grid. The code models the emission of electron (not ion) flows from the plasma emitter and has the ability to include the ionization of the gas in the accelerating gap by electrons, the secondary ion–electron emission from the cathode surface, and the effect of the flow of secondary ions on the emission plasma. The electron fluxes emitted from the meniscus surface are modelled by current tubes, and the fluxes of secondary ions and electrons are determined by

solving the hydrodynamic equations. The potential and electric field distributions in the system are found by solving the Poisson equation by difference methods on a rectangular grid. ELIS code solves self-consistent stationary and quasistationary problems, is module-structured, provides a user-friendly input–output interface, and has, in our view, the potential to model the plasma emitters of positive ions if equipped with appropriate modules. Even as it currently is, its scope includes the most important processes involved in the operation of plasma emitters.

12. Plasma meniscus

As pointed out in Section 10, in a one-dimensional theory the external potential controls the thickness of the unipolar sheath, and the plasma occupies precisely as much of the diode gap as needed to ensure that the emission current j_p is equal to the current $j_{3/2}$ predicted by the Child–Langmuir law. In two dimensions (Fig. 10), the plasma meniscus has its edges tied to the triple point on the outlet hole aperture, so that the diode gap size is to a limited extent controlled by varying the meniscus shape. It is sometimes argued [13, 74, 123] that the meniscus surface will be flat if $j_p = j_{3/2}$, concave toward the plasma if $j_p < j_{3/2}$, and concave outward if $j_p > j_{3/2}$. It is also clear that the meniscus shape affects the focusing of the beam drawn from a plasma emitter. It is assumed that the beam is focused best when the focusing electrode surface looking toward the collector is Pearce-shaped [88, 90, 91, 124 –126] and smoothly matches the plasma meniscus [13], as illustrated in Fig. 10.

While the meniscus shape is extremely difficult to determine experimentally, a well-established fact is that the optimum conditions exist under which the ion beam can be focused best [97, 127]. It is known that the beam cannot be guided through the transport channel if PBGUNS calculations reveal a convexity toward the diode gap on the meniscus near the triple point [127]. The beam is also somewhat defocused if $j_p < j_{3/2}$, and the meniscus displaces into the depth of the outlet hole aperture.

The Debye sheath forms not only on the free plasma surface (i.e., on the plasma meniscus), but also on its boundary, with the focusing electrode within the plasma chamber. The conditions of the formation of these Debye sheaths are very different, however. Whereas ions leave the plasma volume through the free surface virtually alone, the plasma quasineutrality requirement implies that the walls of the plasma chamber are reached predominantly by electrons. Still, because electrons are more mobile than ions, in the Debye sheath near the chamber wall ions are speeded up and electrons slow down, just as in the Debye sheath on a free surface. Hence, the plasma acquires a small positive potential with respect to the chamber walls (with respect to the focusing electrode) and a large positive potential with respect to the ion collector. To reduce the current to the plasma chamber walls, the walls are made magnetically insulated.

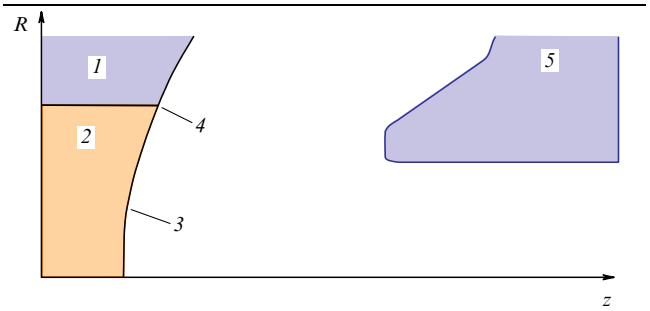

Figure 10. Plasma emitter in a two-dimensional geometry: *1*, focusing electrode; *2*, plasma; *3*, plasma emission surface (plasma meniscus); *4*, triple point; *5*, accelerating electrode. The edges of the plasma meniscus are adjacent to the focusing electrode at the triple point. With the accelerating gap voltage optimized, the plasma meniscus surface goes over smoothly, with no kinks, to that part of the focusing electrode surface that looks toward the ion collector.

Algorithms for calculating the plasma meniscus shape are among the most safely guarded secrets of software code designers. The only paper the authors know of that comes anywhere close to clearly describing them is that of Humphries [74], which presents a method of numerically modeling the plasma emitter of positive ions using the finite element method in combination with the dynamic generation of a triangular conform grid. A feature of the method is that some of the grid elements are considered to belong to the plasma and some to the accelerating gap.

The surface of the meniscus is identified as one bringing together those grid element edges along which the elements of one sort are glued to those of the other. It is argued that such an approach yields high precision, has universality, and is adaptive, a property necessary for calculating complex multi-aperture emission surfaces. The iteration process displaces the grid nodes in such a way as to reduce the nonuniformity of the emission current density on the meniscus surface. The criterion for terminating the iteration process is — as the author postulates without elaboration — that the emission current density become uniform.

An algorithm for calculating the meniscus shape codeveloped by one of us (VTA) within the POISSON-2 framework is worth outlining here in general terms. Unlike Humphries's [74] algorithm, the emission current density j_p is not assumed to be distributed uniformly over the meniscus surface but is calculated in about the same way as in the PBGUNS package. The angular distribution, velocity, and density of ions on the rear wall of the plasma chamber are specified by the user (we do not consider here electron sources which can also be modelled by the POISSON-2 package). Because a quasineutral plasma has no electric field, these ions move ballistically.

This model approximately corresponds to the supersonic ($v_{in} > c_s$) injection of ions into the quasineutral zero-potential ($\varphi = 0$) part of the plasma, a scenario described in Section 9. Some of the trajectories terminate at the inner walls of the plasma chamber, and such ions are considered lost, whereas some others move out to the plasma free surface to form the emission current there, and the density of the emission current j_p turns out to be nonuniform, with j_p on the periphery of the outlet hole usually being lower than on its axis. Choosing a certain value of $\varphi = \varphi_p$, for example, $\varphi_p = -4T_e/e$, as a potential of the plasma free boundary, the equations of Section 9 yield the ion flow velocity v_p and the electric field E_p at this boundary [79].

Outside of the plasma, a thin layer adjacent to its boundary is considered as a planar diode in which the current density is limited by the space charge of the ions drawn from the plasma. The diode thickness d should be specified by the user and is usually equal to two or three difference grid intervals. The voltage U across this diode is determined from the potential calculated in the previous iteration. Given the known values of U, v_p, E_p, and d, the solution of the one-dimensional Poisson equation yields the diode current density $j_{3/2}$, which is used to calculate the parameters

of current tubes in the accelerating gap. Then, as a result of the iteration process, the fields and current tubes in the gap are matched. Once this process is completed, one step of the next iteration process is performed, which causes the nodes of the meniscus to displace. Then, repeating the iteration process results in matching the fields and current tubes, etc. Iterations terminate when j_p becomes identical to $j_{3/2}$.

13. Conclusion

This paper presents, in a single framework, the key results of the one-dimensional theory of a plasma emitter of positive ions. The Bohm criterion is formulated in a simple form and in a generalized form. The theory of a unipolar sheath and the two-scale theory are described, which enable the quantitative determination of the thickness of a collisionless Debye sheath. The kinetic and hydrodynamic formation models of the Debye sheath and of the ionization zone in the Debye presheath are described in an easy-to-access form. It is shown that, except for some artificial ionization models, Bohm's criterion is satisfied in the form of an equality. The emission current from a plasma emitter is calculated in the hydrodynamic and kinetic approximations.

The existing numerical codes for two- and three-dimensional modeling of positive ion sources are briefly discussed, and their critical analysis in light of the analytical theory described in the paper points to the modeling of bulk plasma processes as their least-developed aspect. In particular, the analytical theory predicts that under real-life conditions, the Bohm criterion is satisfied in the form of an equality, and therefore the ion flow velocity at the entrance to the Debye sheath is equal (in the hydrodynamic limit) or close (in kinetic theory) to the ion speed of sound. A positive aspect of these codes, however, is that the initial ion velocity can be prespecified to have an arbitrary value.

Acknowledgments

Financial support from the Russian Science Foundation (project 14-50-00080) is gratefully acknowledged. The authors are grateful to A V Anikeev, Yu I Belchenko, V I Davydenko, A A Ivanov, I V Kandaurov, D I Skovorodin, and A V Sorokin for the helpful discussions of separate issues addressed in the present paper.

References

1. Gabovich M D *Fizika i Tekhnika Plazmennykh Istochnikov Ionov* (Physics and Engineering of Plasma Ion Sources) (Moscow: Atomizdat, 1972)
2. Gabovich M D, Pleshivtsev N V, Semashko N N *Ion and Atomic Beams for Controlled Fusion and Technology* (New York: Consultants Bureau, 1989); Translated from Russian: *Puchki Ionov i Atomov dlya Upravlyaemogo Termoyadernogo Sinteza i Tekhnologicheskikh Tselei* (Moscow: Energoatomizdat, 1986)
3. Gabovich M D *Sov. Phys. Usp.* **20** 134 (1977); *Usp. Fiz. Nauk* **121** 259 (1977)
4. Forrester A T *Large Ion Beams*: *Fundamentals of Generation and Propagation* (New York: Wiley, 1988) Ch. 3; Translated into Russian: *Intensivnye Ionnye Puchki* (Moscow: Mir, 1992)
5. Kreindel' Yu E et al. *Plazmennye Istochniki Elektronov* (Plasma Electron Sources) (Moscow: Energoatomizdat, 1977)
6. Koval' N N et al. *Emissionnaya Elektronika* (Emission Electronics) (Ser. Electronics, Ed. Yu S Protasov) (Emission Electronics) (Moscow: Izd. MGTU im. N E Baumana, 2009)
7. Bohm D "Minimum ionic kinetic energy for a stable sheath", in *The Characteristics of Electrical Discharges in Magnetic Fields* (National Nuclear Energy Ser. Manhattan Project Technical Section, Division I, Vol. 5, Eds A Guthrie, R K Wakerling) (New York: McGraw-Hill, 1949) p. 77–86
8. Chen F F, in *Plasma Diagnostic Techniques* (Pure and Applied Physics, Vol. 21, Eds R H Huddlestone, S L Leonard) (New York: Academic Press, 1965) Ch. 3
9. Chapman B *Glow Discharge Processes*: *Sputtering and Plasma Etching* (New York: Wiley, 1980) Ch. 4
10. Chen F F *Introduction to Plasma Physics and Controlled Fusion* Vol. 1 (New York: Plenum Press, 1984) Ch. 8
11. Lieberman M A, Lichtenberg A J *Principles of Plasma Discharges and Materials Processing* (New York: Wiley, 1994) Ch. 6
12. Chen F F, Chang J P *Lecture Notes on Principles of Plasma Processing* (New York: Kluwer Acad./Plenum Publ., 2003)
13. Humphries S *Charged Particle Beams* (Mineola: Dover Publ., 2013) Ch. 7
14. Stangeby P C *The Plasma Boundary of Magnetic Fusion Devices* (Plasma Physics Series, Vol. 7) (Bristol: Institute of Physics Publ., 2000)
15. Langmuir I *General Electric Rev.* **26** 731 (1923)
16. Langmuir I, Mott-Smith H *General Electric Rev.* **27** 449 (1924)
17. Langmuir I *Proc. Natl. Acad. Sci. USA* **14** 627 (1928)
18. Langmuir I *Phys. Rev.* **33** 954 (1929)
19. Tonks L, Langmuir I *Phys. Rev.* **34** 876 (1929)
20. Kagan Yu M, Perel' V I *Sov. Phys. Usp.* **6** 767 (1964); *Usp. Fiz. Nauk* **81** 409 (1963)
21. Huddlestone R H, Leonard S L (Eds) *Plasma Diagnostic Techniques* (New York: Academic Press, 1965); Translated into Russian: *Diagnostika Plazmy* (Moscow: Mir, 1967)
22. Kozlov O V *Elektricheskii Zond v Plazme* (Electrical Probe in Plasma) (Moscow: Atomizdat, 1969)
23. Lochte-Holtgreven W *Plasma Diagnostics* (Amsterdam: North-Holland, 1968); Translated into Russian: *Metody Issledovaniya Plazmy*: *Spektroskopiya, Lazery, Zondy* (Moscow: Mir, 1971)
24. Davydenko V I, Ivanov A A, Vaisen G *Eksperimental'nye Metody Diagnostiki Plazmy* (Experimental Methods of Plasma Diagnostics) (Novosibirsk: Izd. Tsentr NGU, 1999)
25. Riemann K U, Tsendin L *J. Appl. Phys.* **90** 5487 (2001)
26. Child C D *Phys. Rev. Ser. I* **32** 492 (1911)
27. Langmuir I *Phys. Rev.* **2** 450 (1913)
28. Riemann K U *Phys. Plasmas* **10** 3432 (2003)
29. Caruso A, Cavaliere A *Nuovo Cimento 10* **26** 1389 (1962)
30. Riemann K U *J. Phys. D Appl. Phys.* **24** 493 (1991)
31. Riemann K U *J. Tech. Phys.* **41** 89 (2000)
32. Riemann K U *J. Phys. D Appl. Phys.* **36** 2811 (2003)
33. Riemann K U *Phys. Plasmas* **13** 063508 (2006)
34. Hall L S *Phys. Fluids* **4** 388 (1961)
35. Cohen R H, Ryutov D D *Contrib. Plasma Physics* **44** 111 (2004)
36. Cipolla J W, Silevitch M B *J. Plasma Phys.* **25** 373 (1981)
37. Allen J E *Plasma Sources Sci. Technol.* **18** 014004 (2009)
38. Kotelnikov I A *Lektsii po Fizike Plazmy* (Lectures on Plasma Physics) (Moscow: Binom, 2013)
39. Nikulin S P, in *Trudy 2-go Kreindelevskogo Seminara "Plazmennaya Emissionnaya Elektronika", Ulan-Ude, 17–24 Iyunya 2005 g.* (Proc. of the 2nd Kreindel Workshop "Plasma Emission Electronics", Ulan-Ude, 17–24 June 2005) (2005) pp. 51–53
40. Londer Ya I, Ul'yanov K N *Plasma Phys. Rep.* **39** 849 (2013); *Fiz. Plazmy* **39** 949 (2013)
41. Allen J E, Thonemann P C *Proc. Phys. Soc. B* **67** 768 (1954)
42. Scheuer J T, Emmert G A *Phys. Fluids* **31** 3645 (1988)
43. Godyak V A *Phys. Lett. A* **89** 80 (1982)
44. Godyak V A, Sternberg N *Phys. Rev. A* **42** 2299 (1990)
45. Braun S *Usp. Fiz. Nauk* **133** 693 (1981); Brown S C, in *Gaseous Electronics* Vol. 1 *Electrical Discharges* (Eds M N Hirsh, H J Oskam) (New York: Academic Press, 1978) p. 1
46. Kotelnikov I A *Vestn. NGU* (3) 108 (2008)
47. Franklin R N, Snell J *Phys. Plasmas* **7** 3077 (2000)
48. Franklin R N, Snell J *Phys. Plasmas* **8** 643 (2001)
49. Ul'yanov K N *High Temp.* **38** 344 (2000); *Teplofiz. Vys. Temp.* **38** 367 (2000)

50. Nikulin S P *Russ. Phys. J.* **54** 393 (2011); *Izv. Vyssh. Uchebn. Zaved. Fiz.* (4) 3 (2011)
51. Kino G S, Shaw E K *Phys. Fluids* **9** 587 (1966)
52. Lam S H *Phys. Fluids* **8** 73 (1965)
53. Lam S H *Phys. Fluids* **8** 1002 (1965)
54. Franklin R N, Ockendon J R *J. Plasma Phys.* **4** 371 (1970)
55. Riemann K U *Phys. Plasmas* **4** 4158 (1997)
56. Godyak V, Sternberg N *Phys. Plasmas* **9** 4427 (2002)
57. Allen J E *Phys. Plasmas* **10** 1528 (2003)
58. Tskhakaya D D, Shukla P K *Phys. Plasmas* **10** 3437 (2003)
59. Benilov M S *Phys. Plasmas* **10** 4584 (2003)
60. Franklin R N *Phys. Plasmas* **10** 4589 (2003)
61. Harrison E R, Thompson W B *Proc. Phys. Soc.* **74** 145 (1959)
62. Boyd R L F, Thompson J B *Proc. R. Soc. Lond. A* **252** 102 (1959)
63. Bertotti B, Cavaliere A *Nuovo Cimento 10* **35** 1244 (1965)
64. Allen J E, in *Plasma Physics* Vol. 1 (Ed. B E Keen) (London: Institute of Physics, 1974)
65. Allen J E *J. Phys. D Appl. Phys.* **9** 2331 (1976)
66. Cavaliere A, Engelmann F, Sestero A *Phys. Fluids* **11** 158 (1968)
67. Franklin R N *Plasma Phenomena in Gas Discharges* (Oxford: Clarendon Press, 1976)
68. Prewett P D, Allen J E *Proc. R. Soc. Lond. A* **348** 435 (1976)
69. Braithwaite N St J, Allen J E *J. Phys. D Appl. Phys.* **21** 1733 (1988)
70. Raadu M A, Rasmussen J J *Astrophys. Space Sci.* **144** 43 (1988)
71. Raadu M A *Phys. Rep.* **178** 25 (1989)
72. Baalrud S D, Hegna C C *Phys. Plasmas* **18** 023505 (2011)
73. Dubinov A E, Senilov L A *Tech. Phys.* **57** 1090 (2012); *Zh. Tekh. Fiz.* **82** (8) 50 (2012)
74. Humphries S (Jr.) *J. Comput. Phys.* **204** 587 (2005)
75. Emmert G A et al. *Phys. Fluids* **23** 803 (1980)
76. Riemann K U *Phys. Fluids* **24** 2163 (1981)
77. FAR-TECH Inc. PBGUNS Manual, FAR-TECH, Inc., 2013, http://far-tech.com/pbguns/manuals.html
78. Astrelin V et al., in *15th Intern. Symp. on High-Current Electronics, September 21 – 26, 2008, Tomsk, Russia*
79. Astrelin V T *Usp. Prikl. Fiz.* **1** 574 (2013)
80. Dubinov A E, Senilov L A *Tech. Phys. Lett.* **37** 900 (2011); *Pis'ma Zh. Tekh. Fiz.* **37** (19) 23 (2011)
81. Davydenko V I, Dimov G I, Roslyakov G V *Sov. Phys. Dokl.* **28** 685 (1983); *Dokl. Akad. Nauk SSSR* **271** 1380 (1983)
82. Kotelnikov I A, Skovorodin D I *Fiz. Plazmy* (2015) submitted
83. Abdrashitov G F et al., in *Plasma Science, 1995. IEEE Conf. Record — Abstracts., 1995 IEEE Intern. Conf.* (1995) p. 121
84. Davydenko V I et al. *Rev. Sci. Instrum.* **68** 1418 (1997)
85. Ivanov A A et al. *Rev. Sci. Instrum.* **71** 3728 (2000)
86. Abdrashitov G F et al. *Rev. Sci. Instrum.* **72** 594 (2001)
87. Davydenko V I, Ivanov A A *Rev. Sci. Instrum.* **75** 1809 (2004)
88. Davydenko V I, Ivanov A A, Korepanov S A, Kotelnikov I A *Rev. Sci. Instrum.* **77** 03B902 (2006)
89. Den Hartog D J et al. *Rev. Sci. Instrum.* **77** 10F122 (2006)
90. Davydenko V I, Ivanov A A, Kotelnikov I A, Tiunov M A *Nucl. Instrum. Meth. Phys. Res. A* **576** 259 (2007)
91. Kotelnikov I A t al. *Rev. Sci. Instrum.* **79** 02B702 (2008)
92. Listopad A A et al. *Rev. Sci. Instrum.* **81** 02B104 (2010)
93. Sorokin A et al. *Rev. Sci. Instrum.* **81** 02B108 (2010)
94. Belchenko Yu I et al. *AIP Conf. Proc.* **1515** 167 (2013)
95. Becker R *Rev. Sci. Instrum.* **67** 1132 (1996)
96. Turek M et al. *Instrum. Exp. Tech.* **52** 90 (2009); *Prib. Tekh. Eksp.* (1) 101 (2009)
97. Lawrie S R et al. *Rev. Sci. Instrum.* **81** 02A707 (2010)
98. Miyamoto K et at al. *Appl. Phys. Lett.* **102** 023512 (2013)
99. Il'in V P *Chislennye Metody Resheniya Zadach Elektrofiziki* (Numerical Methods of Solution of Electrophysics Problems) (Moscow: Nauka, 1985)
100. Tozoni O V *Mathematical Models for the Evaluation of Electric and Magnetic Fields* (London: Iliffe, 1968); Translated from Russian: *Matematicheskie Modeli dlya Rascheta Elektricheskikh i Magnitnykh Polei* (Kiev: Naukova Dumka, 1964)
101. Strang G, Fix G J *An Analysis of the Finite Element Method* (Englewood Cliffs, N.J.: Prentice-Hall, 1973); Translated into Russian: *Teoriya Metoda Konechnykh Elementov* (Moscow: Mir, 1977)
102. Grigor'ev Yu N, Vshivkov V A, Fedoruk M P *Chislennoe Modelirovanie Metodami Chastits v Yacheikakh* (Numerical Simulation by Methods of Particles in Cells) (Novosibirsk: Izd. SO RAN, 2004)
103. Whealton J H et al. *J. Appl. Phys.* **64** 6210 (1988)
104. Boers J E, in *Plasma Science, 1993. IEEE Intern. Conf.* (1993) p. 213
105. Boers J E, in *Proc. of the Particle Accelerator Conf., 1995* Vol. 4 (1995) pp. 2312 – 2313
106. Spädtke P, Mühle C *Rev. Sci. Instrum.* **71** 820 (2000)
107. Spädtke P *Rev. Sci. Instrum.* **75** 1643 (2004)
108. Spädtke P, in *The Physics and Technology of Ion Sources* 2nd ed. (Ed. I G Brown) (New York: Wiley, 2006) p. 41 – 60
109. Litovko I V *Cybernetics Syst. Analysis* **44** 780 (2008)
110. Spädtke P "AXCEL code", Ing. Buro fur Naturwissenschaft und Programmentwicklung (1983)
111. Spädtke P "AXCEL-GSI Code", Report GSI GSI-38-9 (1983)
112. Spädtke P, in *Proc. 1984 Linear Accelerator Conf., Seeheim, Germany* (1984) p. 356
113. Astrelin V T, Ivanov V Ya *Avtometriya* **3** 92 (1980)
114. Astrelin V T, Ivanov V Ya, in *Trudy IV Vsecoyuznogo Seminara "Metody Rascheta Elektronno-opticheskikh Sistem"* (Proc. of the 4th All-Union Seminar "Methods of Calculation of Electron-Optical Systems") (Novosibirsk, 1982) p. 10–14
115. Astrelin V T, Ivanov V Ya *Avtometriya* **4** 87 (1982)
116. Astrelin V T et al., in *Zababakhinskie Nauchnye Chteniya: Sbornik Materialov IX Mezhdunarodnoi Konf. Tezisy* (Zababakhin Scientific Readings. Proc. of the 9th Intern. Conf. Abstracts) (Snezhinsk, 2007) p. 115–116
117. Astrelin V T, Kandaurov I V, Trunev Yu A *Tech. Phys.* **59** 258 (2014); *Zh. Tekh. Fiz.* **84** 106 (2014)
118. Astrelin V T, Davydenko V I, Kolmogorov A V *Izv. Vyssh. Ucheb. Zaved. Fiz.* **57** (11-3) 128 (2014)
119. Boris J P, in *Proc. of the 4th Conf. on Numerical Simulation of Plasmas* (Washington, D.C.: Naval Res. Lab., 1970) pp. 3 – 67
120. Petrovich O N, Gruzdev V A *Priklad. Fiz.* **2** 79 (2012)
121. Petrovich O N "Modelirovanie elektronno-opticheskikh sistem s plazmennym emitterom" ("Simulation of electron-optical systems with a plasma emitter"), PhD Thesis of Engineering Sciences (Novopolotsk, Belarus: Polotsk State Univ., 2013)
122. Sveshnikov V M, Zalesskii V G, Petrovich O N *Priklad. Fiz.* (2) 40 (2012)
123. Kenichi A et al. *Jpn. J. Appl. Phys.* **15** 1343 (1976)
124. Pierce J R *J. Appl. Phys.* **11** 548 (1940)
125. Pierce J R *Theory and Design of Electron Beams* (New York: Van Nostrand, 1954)
126. Radley D E *J. Electron. Control* **4** 125 (1958)
127. Sorokin A V (2015) Private communication